

Fluctuations, dissipation and the dynamical Casimir effect

Diego A. R. Dalvit, Paulo A. Maia Neto, and Francisco Diego Mazzitelli

Abstract Vacuum fluctuations provide a fundamental source of dissipation for systems coupled to quantum fields by radiation pressure. In the dynamical Casimir effect, accelerating neutral bodies in free space give rise to the emission of real photons while experiencing a damping force which plays the role of a radiation reaction force. Analog models where non-stationary conditions for the electromagnetic field simulate the presence of moving plates are currently under experimental investigation. A dissipative force might also appear in the case of uniform relative motion between two bodies, thus leading to a new kind of friction mechanism without mechanical contact. In this paper, we review recent advances on the dynamical Casimir and non-contact friction effects, highlighting their common physical origin.

1 Introduction

The Casimir force discussed in this volume represents the average radiation pressure force upon one of the interacting bodies. When the zero-temperature limit is considered, the average is taken over the vacuum field state. Although the average electric and magnetic fields vanish, the Casimir force is finite because radiation pressure is quadratic in the field strength operators. In this sense, the Casimir force derives from

Diego A. R. Dalvit
Theoretical Division MS B213, Los Alamos National Laboratory, Los Alamos, NM 87545, USA
e-mail: dalvit@lanl.gov

Paulo A. Maia Neto
Instituto de Física UFRJ, Caixa Postal 68528, Rio de Janeiro RJ 21941-972, Brazil
e-mail: pamn@if.ufrj.br

Francisco Diego Mazzitelli
Departamento de Física, FCEyN, Universidad de Buenos Aires and IFIBA, CONICET, Ciudad Universitaria, Pabellón I, 1428 Buenos Aires, Argentina
e-mail: fmazzi@df.uba.ar

the fluctuating fields associated with the field zero-point energy (or more precisely from their modification by the interacting bodies).

As any quantum observable, the radiation pressure itself fluctuates [1, 2]. For a single body at rest in empty space, the average vacuum radiation pressure vanishes (for the ground-state field cannot be an energy source), and all that is left is a fluctuating force driving a quantum Brownian motion [3]. The resulting dynamics is characterized by diffusion in phase space, thus leading to decoherence of the body center-of-mass [4].

Besides diffusion, the radiation pressure coupling also leads to dissipation, with the corresponding coefficients connected by the fluctuation-dissipation theorem [5]. As in the classical Brownian motion, the fluctuating force on the body at rest is closely related to a dissipative force exerted when the body is set in motion. Since the vacuum state is Lorentz invariant, the Casimir dissipative force vanishes in the case of uniform motion of a single body in empty space, as expected from the principle of relativity. For a non-relativistic “mirror” in one spatial dimension (1D), the Casimir dissipative force is proportional to the second-order derivative of the velocity [6], like the radiation reaction force in classical electrodynamics. Casimir dissipation is in fact connected to the emission of photon pairs by the accelerated (electrically neutral) mirror, an effect known as the dynamical Casimir effect (DCE). The power dissipated in the motion of the mirror is indeed equal to the total radiated power in DCE as expected from energy conservation.

The creation of photons in a 1D cavity with one moving mirror was first analyzed by Moore [7], and explicit results were later derived in Ref. [8]. Relativistic results for the dissipative Casimir force upon a single mirror in 1D and the connection with DCE were derived in a seminal paper by Fulling and Davies [9]. At this earlier stage, the main motivation was the analogy with the Hawking radiation associated with black-hole evaporation [10].

The interplay between Casimir dissipation and fluctuations was investigated only much later [3, 11, 12], in connection with a major issue in quantum optics: the fundamental quantum limits of position measurement (this was motivated by the quest for interferometric detection of gravitational waves) [13]. Linear response theory [14] provides a valuable tool for computing the Casimir dissipative force on a moving body from the fluctuations of the force on the body at rest, which is in general much simpler to calculate. This method was employed to compute the dissipative force on a moving, perfectly reflecting sphere [15] and on a plane surface experiencing a time-dependent perturbation [16] (the latter was also computed by taking the full time-dependent boundary conditions (b.c.) [17, 18]).

In all these configurations, Casimir dissipation turns out to be very small when realistic physical parameters are taken into account. The predicted orders of magnitude are more promising when considering a closely related effect: quantum non-contact friction in the shear relative motion between two parallel surfaces [19, 20]. In contrast with the radiation reaction dissipative effect discussed so far, quantum friction takes place even for a uniform relative motion. On the other hand, quantum friction requires the material media to have finite response times (dispersion). From

Kramers-Kronig relations [21], the material media must also be dissipative, and the resulting friction depends on the imaginary part of the dielectric constant ϵ .

Whereas the direct measurement of the Casimir radiation reaction dissipative force seems to be beyond hope, the corresponding photon emission effect might be within reach in the near future. The properties of the radiated photons have been analyzed in great detail over recent years. For a single moving plane mirror, the frequency spectrum was computed in 1D [22] as well as in 3D [23] in the non-relativistic approximation. A variety of 3D geometries were considered, including deforming mirrors [24], parallel plates [25], cylindrical waveguides [26], and spherical cavities containing either scalar [27] or electromagnetic fields [28, 29].

Closed rectangular [30, 31, 32] or cylindrical [33] microwave cavities with one moving wall are by far the best candidates for a possible experimental implementation, with the mechanical oscillation frequency Ω tuned into parametric resonance with cavity field modes. Because of the parametric amplification effect, it is necessary to go beyond the perturbative approximation in order to compute the intracavity photon number even in the non-relativistic regime [34, 35, 36].

As the microwave field builds up inside the cavity, cavity losses (due to transmission, dissipation or diffraction at the rough cavity walls) become increasingly important. Finite transmission at the mirrors of a 1D cavity was taken into account within the scattering approach developed in Refs. [22, 37, 38]. Master equations for the reduced density operator of the cavity field in lossy 3D cavities were derived in Refs. [39, 40]. Predictions for the total photon number produced at very long times obtained from the different models are in disagreement, so that a reliable estimation of the DCE magnitude under realistic conditions is still an open theoretical problem.

It is nevertheless clear that measuring DCE photons is a highly non-trivial challenge (see for instance the proposal [41] based on superradiance amplification). For this reason, in recent years the focus has been re-oriented towards analog models of DCE. Although dynamical Casimir photons are in principle emitted even in the case of a global ‘center-of-mass’ oscillation of a cavity, the orders of magnitude are clearly more favorable when some cavity length is modulated. In this case, one might modulate the optical cavity length by changing the intracavity refractive index (or more generally material optical constants) instead of changing the physical cavity length. For instance, the conductivity of a semiconductor slab can be rapidly changed with the help of a short optical pulse, simulating the motion of a metallic mirror [42, 43] and thereby producing photons exactly as in the DCE [44, 45]. An experiment along these lines is currently under way [46] (see Ref. [47] for an update). Alternatively, one might select a setup for operation of an optical parametric oscillator such that it becomes formally equivalent to DCE with a modulation frequency in the optical domain [38].

Alongside the examples in quantum and nonlinear optics, one can also devise additional analogues of DCE in the field of circuit quantum electrodynamics [48]. For instance, a co-planar waveguide with a superconducting quantum interference device (SQUID) at its end is formally equivalent to a 1D model for a single mirror [49, 50]. When a time-dependent magnetic flux is applied to the SQUID, it simulates the motion of the mirror. More generally, Bose-Einstein condensates also

provide interesting analogues for DCE [51] and Casimir-like dissipation [52], with electromagnetic vacuum fluctuations replaced by zero-point fluctuations of the condensate.

Reviews on fluctuations and Casimir dissipation on one hand and on DCE on the other hand can be found in Refs. [53, 54] and Refs. [55, 56, 57], respectively. This review paper is organized as follows. In Sec. 2, we discuss the interplay between fluctuations, dissipation and the photon creation effect for a single mirror in free space. Sec. 3 presents a short introduction to non-contact quantum friction. In Sec. 4, photon creation in resonant cavities with either moving walls or time-dependent material properties is presented in detail. Sec. 5 briefly discusses experimental proposals, and Sec. 6 contains some final remarks.

2 Dissipative effects of the quantum vacuum

2.1 1D models

We start with the simplest theoretical model: a non-relativistic point-like ‘mirror’ coupled to a massless scalar field $\phi(x, t)$ in 1D. We take the Dirichlet b.c. at the instantaneous mirror position $q(t)$:

$$\phi(q(t), t) = 0. \quad (1)$$

In the non-relativistic approximation, we expect the vacuum radiation pressure force $f(t)$ to be proportional to some derivative of the mirror’s velocity. As a quantum effect, the force must also be proportional to \hbar , and then dimensional analysis yields

$$f(t) \propto \frac{\hbar q^{(3)}(t)}{c^2}, \quad (1D) \quad (2)$$

where $q^{(n)}(t) \equiv d^n q(t)/dt^n$. Note that (2) is consistent with the Lorentz invariance of the vacuum field state, which excludes friction-like forces proportional to $q^{(1)}(t)$ for a single moving mirror (but not in the case of relative motion between two mirrors discussed in the next two sections).

In order to compute the dimensionless prefactor in (2), we solve the b.c. (1) to first order in $q(t)$ as in Ref. [6], with the mirror’s motion treated as a small perturbation. However, instead of analyzing in the time domain, we switch to the frequency domain, which allows us to understand more clearly the region of validity of the theoretical model leading to (2). We write the Fourier transform of the field as a perturbative expansion:

$$\Phi(x, \omega) = \Phi_0(x, \omega) + \delta\Phi(x, \omega), \quad (3)$$

where the unperturbed field $\Phi_0(x, \omega)$ corresponds to a static mirror at $x = 0$: $\Phi_0(0, \omega) \equiv 0$. The boundary condition for $\delta\Phi(x, \omega)$ is derived from (1) by taking a Taylor expansion around $x = 0$ to first order in $Q(\Omega)$ (Fourier transform of $q(t)$):

$$\delta\Phi(0, \omega_0) = - \int_{-\infty}^{\infty} \frac{d\omega_1}{2\pi} Q(\omega_0 - \omega_1) \partial_x \Phi_0(0, \omega_1). \quad (4)$$

Eq. (4) already contains the frequency modulation effect at the origin of Casimir dissipation: the motion of the mirror (frequency Ω) generates an output amplitude at the sideband frequency $\omega_0 = \omega_1 + \Omega$ proportional to $Q(\Omega)$ from a given input field frequency ω_1 .

In order to find the Casimir dissipative force, we take the Fourier transform of the appropriate component $T_{11} = \frac{1}{2}[\frac{1}{c^2}(\partial_t \phi)^2 + (\partial_x \phi)^2]$ of the energy-momentum tensor and then replace the total field $\Phi(x, \omega)$ containing the solution $\delta\Phi(x, \omega)$ of eq. (4). After averaging over the vacuum state, the resulting force is written as

$$F(\Omega) = \chi(\Omega)Q(\Omega), \quad (5)$$

$$\chi(\Omega) = 2i \frac{\hbar}{c^2} \int_{-\infty}^{\infty} \frac{d\omega_1}{2\pi} (\Omega + \omega_1) |\omega_1|. \quad (6)$$

After regularization, it is simple to show that the contribution $\int_{-\infty}^{-\Omega} d\omega_1(\dots)$ cancels the contribution $\int_0^{\infty} d\omega_1(\dots)$ in (6). Thus, only field frequencies in the interval $-\Omega \leq \omega_1 \leq 0$ contribute to the dynamical radiation pressure force, yielding

$$F(\Omega) = i \frac{\hbar \Omega^3}{6\pi c^2} Q(\Omega), \quad (7)$$

in agreement with (2) with a positive prefactor ($\frac{1}{6\pi}$) as expected for a dissipative force. This result was first obtained in Ref. [6] within the perturbative approach and coincides with the non-relativistic limit of the exact result derived much earlier in Ref. [9]. It may also be obtained as a limiting case of the result for a partially transmitting mirror, which was derived either from the perturbative approach outlined here [12] or by developing the appropriate Schwinger-Keldysh effective action within a functional approach to the dissipative Casimir effect [58]. When considering a moving dielectric half-space, one obtains as expected one-half of the r.h.s. of (7) in the limit of an infinite refractive index [59]. The final result for $F(\Omega)$ is exactly the same as in (7) when we replace the Dirichlet b.c. (1) by the Neumann b.c. at the instantaneously co-moving Lorentz frame (primed quantities refer to the co-moving frame) $\partial_{x'} \phi|_{x'=q(t')} = 0$ [60]. Dirichlet and Neumann b.c. also yield the same force in the more general relativistic regime [61]. On the other hand, for the Robin b.c.

$$\partial_{x'} \phi|_{x'=q(t')} = \frac{1}{\beta} \phi|_{x'=q(t')} \quad (8)$$

(β is a constant parameter), the force susceptibility $\chi(\Omega)$ displays a non-monotonic dependence on Ω , and is nearly suppressed at $\Omega \sim 2.5c/\beta$ [62].

We could have anticipated that high-frequency modes with $\omega_i \gg \Omega$ would not contribute because they “see” the mirror’s motion at frequency Ω as a quasi-static perturbation, and indeed the dissipative Casimir force originates from low-frequency modes for which the motion is non-adiabatic. But there is a more illuminating interpretation that explains why the contribution comes precisely from the frequency interval $[-\Omega, 0]$. In Fig. 1, we show that this interval corresponds to the field modes leading to frequency sidebands $\omega_o = \omega_i + \Omega$ (see eq. (4)) *across* the border between positive and negative frequencies (for $\Omega < 0$ the corresponding interval is $[0, -\Omega]$ and the analysis is essentially the same). In other words, for these specific modes the motional frequency modulation leads to mixing between positive and negative frequencies. Bearing in mind the correspondence between positive (negative) frequencies and annihilation (creation) operators, this mixing translates into a Bogoliubov transformation coupling output annihilation operators to input creation ones, and viceversa [63] (examples will be presented in Section 4). The important conclusion is that sideband generation for these modes corresponds to photon creation (and also annihilation in the case of a general initial field state), whereas outside the interval $[-\Omega, 0]$, where no mixing occurs, the sideband effect corresponds to photon inelastic scattering with neither creation nor annihilation.

From this discussion, we can also surmise the important property that the dynamical Casimir photons have frequencies bounded by the mechanical frequency Ω , as long as the perturbative non-relativistic approximation holds [22]. Moreover, the Casimir photons are emitted in pairs, with photon frequencies satisfying $\omega_1 + \omega_2 = \Omega$. Hence the frequency spectrum is symmetrical around $\Omega/2$, where it has a maximum for the Dirichlet case [22] but not generally for the Robin b.c. [64].

In short, the derivation of (2) from (4) highlights the direct connection between the dissipative dynamical force and the dynamical Casimir photon emission effect. The dissipative force thus plays the role of a Casimir radiation reaction force, damping the mirror’s mechanical energy as Casimir photons are emitted. In fact, the expression given by (2) has the same form as the radiation reaction force in classical

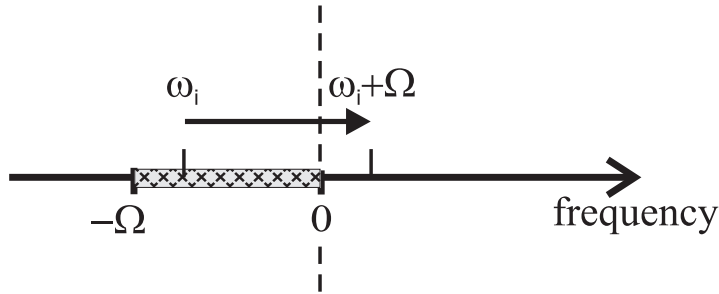


Fig. 1 For a given mechanical modulation frequency Ω (assumed to be positive in this diagram), the field modes contributing to the dissipative dynamical Casimir effect lie in the interval $[-\Omega, 0]$, which corresponds to negative input field frequencies ω_i , yielding positive sideband frequencies.

electrodynamics, apart from a dimensionless pre-factor inversely proportional to the fine-structure constant $e^2/(\hbar c)$.

The discussion on the field modes actually contributing in (4) also allows us to address the domain of validity of the various assumptions employed in the derivation presented above. We have assumed in (1) that the field vanishes at the instantaneous mirror's position, no matter how fast the mirror and field oscillate. However, the electric currents and charge density inside a real metallic mirror respond to field and position changes over a finite time scale, so that we expect our oversimplified model to be physically meaningful only at low frequencies (more general results and discussions are presented in Refs. [12, 65]). Since the relevant field frequencies are bounded by the mechanical frequencies ($|\omega_i| \leq |\Omega|$), the model is consistent as long as typical mechanical frequencies are much smaller than the frequency scales characterizing the metallic response - typically the plasma frequency of metals.

A second point to be clarified is the connection between the perturbative linear approximation employed above and the non-relativistic approximation. When deriving (4) from (1), we have taken the long-wavelength approximation to expand the field around $x = 0$. Let us assume, to simplify the discussion, that the mirror oscillates with frequency Ω and amplitude q_0 . The non-relativistic regime then translates into $\Omega q_0/c \ll 1$ and all relevant field modes correspond to long wavelengths $2\pi c/\omega_i \gg q_0$ since they satisfy the inequality $|\omega_i| \leq \Omega$. More generally, the long-wavelength approximation follows from the non-relativistic condition provided that there is an inertial reference frame for which the motion is spatially bounded.

2.2 Casimir-driven decoherence

As in classical Brownian motion, the dissipative effect is closely related to the fluctuations provided by the reservoir, which in our case is the quantum vacuum field. This connection provides yet another tool for computing the dissipative Casimir force: by using linear response theory, one can derive (7) from the correlation function of the force on a static plate [12]. (This method has been employed for different geometries in 3D [11, 15, 16, 26]). More interestingly, if we take the mirror's position as a full dynamical observable rather than a prescribed function of time, vacuum radiation pressure plays the role of a Langevin fluctuating force [3, 58], leading to diffusion in phase space, which adds to the associated average dissipative force (7).

Let us first analyze the mechanical effect of the dissipative Casimir force in the context of classical dynamics. We consider a point-like mirror of mass M in a harmonic potential well of frequency Ω . Taking the Casimir dissipative force given by (7) into account, and neglecting for the time being any associated stochastic force, we write the mirror's equation of motion as

$$\frac{d^2 q(t)}{dt^2} = -\Omega^2 q(t) + \frac{\hbar}{6\pi M c^2} \frac{d^3 q(t)}{dt^3}. \quad (9)$$

We assume that the oscillator's zero-point energy $\hbar\Omega/2$ is much smaller than the rest mass energy Mc^2 , and then find oscillatory solutions of (9) which are damped at the rate

$$\Gamma = \frac{1}{12\pi} \frac{\hbar\Omega}{Mc^2} \Omega \ll \Omega. \quad (10)$$

This result provides a good illustration of how weak the Casimir dissipation is for a single mirror in a vacuum. On the other hand, the associated diffusion in phase space is more relevant, particularly in the context of the full quantum theory discussed below, since it provides an efficient decoherence mechanism for non-classical quantum states.

The quantum description of the mirror's dynamics can be developed from the Hamiltonian for the radiation pressure coupling with a dispersive semi-transparent mirror (transparency frequency ω_c) [66]. One derives a master equation for the reduced density operator ρ of the mirror, which can also be cast in the form of a Fokker-Planck equation for the Wigner function $W(x, p, t)$ representing the mirror quantum state [4]:

$$\partial_t W = -(1 - \Delta M/M) \frac{p}{M} \partial_x W + M\Omega^2 x \partial_p W + 2\Gamma \partial_x(xW) + D_1 \frac{\partial^2 W}{\partial x^2} - D_2 \frac{\partial^2 W}{\partial x \partial p}. \quad (11)$$

The time-dependent coefficients ΔM (mass correction), Γ (damping coefficient), D_1 and D_2 (diffusion coefficients) are written in terms of the correlation function of the field linear momentum operator. The perfectly reflecting limit corresponding to (1) is obtained when $\Omega \ll \omega_c$, in line with our previous discussion since $1/\omega_c$ represents the characteristic time scale for the material medium response. In this limit, for $t \gtrsim 1/\omega_c$, $\Gamma(t)$ rapidly approaches the expected constant value as given by (10), whereas $D_1(t)$ approaches the asymptotic value

$$D_1 = \hbar\Gamma/(M\Omega) \quad (12)$$

for $t \gtrsim 2\pi/\Omega$. This connection between diffusion and damping plays the role of a fluctuation-dissipation theorem for the vacuum state (zero temperature).

Under the time evolution described by the Fokker-Planck equation (11), an initially pure state gradually evolves into a statistical mixture. The physical reason behind this decoherence effect is the buildup of entanglement between the mirror and the field due to the radiation pressure coupling and the associated dynamical Casimir photon creation [4]. As an example of initial state, we consider the ‘‘Schrödinger’s cat’’ superposition of coherent states $|\psi\rangle = (|\alpha\rangle + |-\alpha\rangle)/\sqrt{2}$ with the amplitude $\alpha = iP_0/\sqrt{2M\hbar\omega_0}$ along the imaginary axis ($\pm P_0$ are the average momenta corresponding to each state’s component). The corresponding Wigner function $W(x, p)$ contains an oscillating term proportional to $\cos(2P_0x/\hbar)$ which represents the coherence of the superposition. Clearly, the diffusion term proportional to D_1 in (11) will wash out these oscillations along the position axis, thus transforming the cat state into a mixture of the two coherent states. From (11) and (12), the corresponding decoherence time scale is

$$t_d = \frac{\hbar^2}{2P_0^2 D_1} = 4 \left(\frac{\delta p}{2P_0} \right)^2 \Gamma^{-1}, \quad (13)$$

where $\delta p = \sqrt{M\hbar\Omega/2}$ is the momentum uncertainty of the coherent state (we have assumed that $\Omega t_d \gg 1$). Since $2P_0$ measures the distance between the two components in phase space, (13) shows that decoherence is stronger when the state components are further apart, corresponding to thinner interference fringes in phase space. Decoherence from entanglement driven by dynamical Casimir photon creation is thus very effective for macroscopic superpositions in spite of the smallness of the corresponding damping coefficient Γ . As the radiation pressure control of microresonators improves all the way to the quantum level [67], Casimir driven decoherence might eventually become of experimental relevance.

2.3 3D models

The orders of magnitude can be reliably assessed only by considering the real-world three-dimensional space. We start with the simplest geometry in 3D: a plane mirror parallel to the xy plane, of area A and moving along the z -axis. For an infinite plane, we expect the dissipative Casimir force to be proportional to A , so that we have to modify (2) to include a squared length. For a scalar field satisfying a Dirichlet b.c. analogous to (1), the derivation is very similar to the one outlined above [6]:

$$f(t) = -\frac{\hbar A q^{(5)}(t)}{360\pi^2 c^4}. \quad (3\text{D, scalar}) \quad (14)$$

For the electromagnetic field, the model of perfect reflectivity provides an accurate description of metallic mirrors at low frequencies. For a mirror moving along the z -axis, the electric and magnetic fields in the instantaneously co-moving Lorentz frame S' satisfy

$$\hat{\mathbf{z}} \times \mathbf{E}'|_{\text{mirror}} = 0, \quad \hat{\mathbf{z}} \cdot \mathbf{B}'|_{\text{mirror}} = 0. \quad (15)$$

It is useful to decompose the fields into transverse electric (TE) and transverse magnetic (TM) polarizations (where ‘transverse’ means perpendicular to the incidence plane defined by $\hat{\mathbf{z}}$ and the propagation direction). For the TE component, we define the vector potential in the usual way: $\mathbf{E}^{(\text{TE})} = -\partial_t \mathbf{A}^{(\text{TE})}$, $\mathbf{B}^{(\text{TE})} = \nabla \times \mathbf{A}^{(\text{TE})}$ under the Coulomb gauge $\nabla \cdot \mathbf{A}^{(\text{TE})} = 0$. Since $\mathbf{A}^{(\text{TE})} \cdot \hat{\mathbf{z}} = 0$, $\mathbf{A}^{(\text{TE})}$ is invariant under the Lorentz boost from the co-moving frame to the laboratory frame. The resulting b.c. is then similar to (1):

$$\mathbf{A}^{(\text{TE})}(x, y, q(t), t) = \mathbf{0}. \quad (16)$$

On the other hand, $\mathbf{A}^{(\text{TM})}$ has a component along the z -axis, so that the Coulomb gauge is no longer invariant under the Lorentz boost, resulting in complicated b.c. also involving the scalar potential. It is then convenient to define a new vector potential $\mathcal{A}^{(\text{TM})}$ as

$$\mathbf{E}^{(\text{TM})} = \nabla \times \mathcal{A}^{(\text{TM})}, \quad \mathbf{B}^{(\text{TM})} = \partial_t \mathcal{A}^{(\text{TM})}$$

under the gauge $\nabla \cdot \mathcal{A}^{(\text{TM})} = 0$. Like $\mathbf{A}^{(\text{TE})}$, $\mathcal{A}^{(\text{TM})}$ is also invariant under Lorentz boosts along the z -axis. From (15), one derives that $\mathcal{A}^{(\text{TM})}$ satisfies a Neumann b.c. at the co-moving frame, yielding

$$[\partial_z + \dot{q}(t)\partial_t + \mathcal{O}(\dot{q}^2)] \mathcal{A}^{(\text{TM})}(x, y, q(t), t) = \mathbf{0}. \quad (17)$$

The condition of perfect reflectivity then results in two independent problems: a Dirichlet b.c. for TE modes, and a Neumann b.c. in the instantaneously co-moving frame for TM modes. The TM contribution turns out to be 11 times larger than the TE one, which coincides with (14). The resulting dissipative force is then [68]

$$f(t) = -\frac{\hbar A q^{(5)}(t)}{30\pi^2 c^4}. \quad (3\text{D, electromagnetic}) \quad (18)$$

As in the 1D case, the dissipative Casimir force plays the role of a radiation reaction force, associated with the emission of photon pairs with wave-vectors satisfying the conditions $|\mathbf{k}_1| + |\mathbf{k}_2| = \Omega/c$ and $\mathbf{k}_{1\parallel} = -\mathbf{k}_{2\parallel}$ from translational symmetry parallel to the plane of the mirror. The angular distribution of emitted photons displays an interesting correlation with polarization: TE photons are preferentially emitted near the normal direction, whereas TM ones are preferentially emitted at larger angles, near a grazing direction if the frequency is smaller than $\Omega/2$ [23].

Results beyond the model of perfect reflection were obtained in Ref. [69] for a dielectric half-space (see also Ref. [70] for the angular and frequency spectra of emitted photons). In this case, there is also photon emission (and the associated dissipative radiation reaction force) if the dielectric mirror moves sideways, or if a dielectric sphere rotates around a diameter [71]. We will come back to this type of arrangement when discussing non-contact quantum friction in the next section.

To conclude this section, we compute the total photon production rate for a perfectly reflecting oscillating mirror directly from (18). By energy conservation, the total radiated energy is the negative of the work done on the mirror by the dissipative Casimir force:

$$E = -\int_{-\infty}^{\infty} f(t) q^{(1)}(t) dt. \quad (19)$$

We evaluate the integral in (19) using the result (18) for an oscillatory motion of frequency Ω and amplitude q_0 exponentially damped over a time scale $T \gg 1/\Omega$: $E = \hbar T A q_0^2 \Omega^6 / (120\pi^2 c^4)$. Since the spectrum is symmetrical with respect to the frequency $\Omega/2$, we can derive the number of photons N from the radiated energy using the relation $E = N\hbar\Omega/2$. The total photon production rate is then given by

$$\frac{N}{T} = \frac{1}{15} \frac{A}{\lambda_0^2} \left(\frac{v_{\text{max}}}{c} \right)^2 \Omega \quad (20)$$

with $v_{\max} \equiv \Omega q_0$ and $\lambda_0 \equiv 2\pi c/\Omega$ representing the typical scale of the relevant wavelengths. With $v_{\max}/c \sim 10^{-7}$, $\Omega/(2\pi) \sim 10$ GHz and $A \sim \lambda_0^2 \sim 10\text{cm}^2$, we find $N/T \sim 10^{-5}$ photons/sec or approximately one photon pair every two days!

The dynamical Casimir effect is clearly very small for a single oscillating mirror. Adding a second parallel plane mirror, the photon production rate is enhanced by a factor $(\Omega L/c)^{-2} \sim 10^6$ for separation distances L in the sub-micrometer range [25]. But at such short distances, finite conductivity of the metallic plates, not considered so far, is likely to reduce the photon production rate. In this type of arrangement, a much larger effect is obtained by considering the shear motion of one plate relative to the other (instead of a relative motion along the normal direction). As discussed in the next section, because of finite conductivity a large friction force is predicted at short distances, which results from the creation of pairs of excitations inside the metallic medium [20, 72]. As for the emission of photon pairs, the orders of magnitude are more promising when considering a closed cavity with moving walls, to be discussed in Section 4.

3 Quantum Friction

There is an intimate connection between the dynamical Casimir effect and the possibility that electrically neutral bodies in relative motion may experience non-contact friction due to quantum vacuum fluctuations, the so-called “quantum friction”. As we have discussed in the previous section, dielectric bodies in accelerated motion radiate Casimir photons. Shear motion of two bodies, even at constant relative speed, can also radiate energy. Just as in the case of a single accelerated mirror in a vacuum, shear motion cannot be removed by a change of reference frame. A frictional force between two perfectly smooth parallel planes shearing against each other with a relative velocity \mathbf{v} results from the exchange of photons between the two surfaces. These photons carry the information of the motion of one surface to the other one, and as a result linear momentum is exchanged between the plates, leading to friction.

In order to illustrate the physics of quantum friction we will follow here an approach due to Pendry [20] who considered the simplest case of zero temperature and the non-retarded (van der Waals) limit. The nice feature of this approach is that it manifestly connects to the intuitive picture of motion-induced (virtual) photons as mediators of momentum exchange between the shear surfaces. A dielectric surface, although electrically neutral, experiences quantum charge fluctuations, and these have corresponding images on the opposing dielectric surface. Since the surfaces are in relative parallel motion, the image lags behind the fluctuating charge distribution that created it, and this results in a frictional van der Waals force. Note that for ideal perfect metals, the image charges arrange themselves instantaneously (do not lag behind), and therefore no quantum friction is expected in this case.

We model each of the dielectric surfaces as a continuum of oscillators with Hamiltonian

$$\hat{H}_\alpha = \sum_{\mathbf{k}j} \hbar \omega_{\alpha;\mathbf{k}j} (\hat{a}_{\alpha;\mathbf{k}j}^\dagger \hat{a}_{\alpha;\mathbf{k}j} + 1/2), \quad (21)$$

where $\hat{a}_{\alpha;\mathbf{k}j}^\dagger$ and $\hat{a}_{\alpha;\mathbf{k}j}$ are creation and annihilation bosonic operators associated with the upper ($\alpha = u$) or lower ($\alpha = l$) plate. Each mode on each surface is defined by \mathbf{k} , which is a wave-vector parallel to the planar surface, and by j , which denotes degrees of freedom perpendicular to the surface. Following Pendry we restrict ourselves to the non-retarded limit (very long wavelengths for the EM modes). In this limit the EM field is mainly electrostatic, only the static TM polarization matters for a dielectric surface (since the static TE field is essentially a magnetic field that does not interact with the non-magnetic surface), and the intensity decays exponentially from the surfaces (evanescent fields). The coupling between the oscillator modes belonging to different surfaces is mediated by the EM field, and it is assumed to be a position-position interaction of the form

$$\hat{H}_{\text{int}}(t) = \sum_{\mathbf{k}j j'} C_{\mathbf{k}j j'}(d) \hat{x}_{u;\mathbf{k}j} \otimes \hat{x}_{l;-\mathbf{k}j'} e^{-ik_x vt}. \quad (22)$$

In the non-relativistic limit the effect of the surfaces shearing with speed v along the x direction is contained in the last exponential factor. This type of Hamiltonian follows from the effective electrostatic interaction between the fluctuating charges in the dielectrics and its expansion to lowest order in the displacement of each oscillator from its equilibrium position (equivalently, it also follows from the non-retarded and static limit of the dipole-dipole interactions between fluctuating dipoles in each surface). The coupling factors $C_{\mathbf{k}j j'}(d)$ can be obtained by analyzing how each oscillator dissipates energy into the vacuum gap. This is done in Ref. [20] in two ways, by invoking a scattering type of approach relating the fields at the interphases with reflection amplitudes, and by considering how the fluctuating charge distributions in each surface dissipate energy. The result is $C_{\mathbf{k}j j'}(d) = (\beta_{\mathbf{k}j} \beta_{\mathbf{k}j'} / 2k\epsilon_0) e^{-|\mathbf{k}|d}$, where

$$\beta_{\mathbf{k}j}^2 = \left(\frac{dN}{d\omega} \right)^{-1} \frac{4k\omega\epsilon_0}{\pi} \text{Im} \left[\frac{\epsilon(\omega) - 1}{\epsilon(\omega) + 1} \right]. \quad (23)$$

Note the exponential decay due to the evanescent nature of the EM field. In this equation $dN/d\omega$ is the density of oscillator modes at frequency ω and $\epsilon(\omega)$ is the complex dielectric permittivity of the plates (assumed to be identical). Although the interaction Hamiltonian does not depend explicitly on the quantized EM field (because this derivation is semiclassical), one can infer the quantum processes of creation and absorption that take place by expanding the product $\hat{x}_{u;\mathbf{k}j} \otimes \hat{x}_{l;-\mathbf{k}j'}$:

$$\hat{x}_{u;\mathbf{k}j} \otimes \hat{x}_{l;-\mathbf{k}j'} = -\frac{1}{2} [\hat{a}_{u;\mathbf{k}j}^\dagger - \hat{a}_{u;\mathbf{k}j}] \otimes [\hat{a}_{l;-\mathbf{k}j'}^\dagger - \hat{a}_{l;-\mathbf{k}j'}]. \quad (24)$$

Imagine the system of the two dielectrics is initially in the ground state at zero temperature, $|\psi(t=0)\rangle = |\psi_g\rangle_u \otimes |\psi_g\rangle_l$, where $|\psi_g\rangle_\alpha = \prod_{\mathbf{k}j} |\psi_{g,\mathbf{k}j}\rangle_\alpha$ is the product of the harmonic oscillators' ground states for surface α . Eq.(24) implies that two motion-induced virtual photons created from an EM vacuum produce one

excitation in each surface, i.e., there is a non-zero probability of transition to states $|1; \mathbf{k}j\rangle_u \otimes |1; -\mathbf{k}j'\rangle_l$. The transition probability can be computed using time-dependent perturbation theory for the perturbation $H_{\text{int}}(t)$. To first order, the transition probability from the ground state into each of these two-excitation states is

$$P_{\mathbf{k}j j'}(t) = \frac{\beta_{\mathbf{k}j}^2 \beta_{\mathbf{k}j'}^2}{4k^2 \varepsilon_0^2} \frac{e^{-2d|\mathbf{k}|}}{4\omega_{u,\mathbf{k}j}\omega_{l,-\mathbf{k}j'}} \frac{4 \sin^2[(\omega_{u,\mathbf{k}j} + \omega_{l,-\mathbf{k}j'} - k_x v)t/2]}{(\omega_{u,\mathbf{k}j} + \omega_{l,-\mathbf{k}j'} - k_x v)^2}. \quad (25)$$

In the limit of large times ($t \rightarrow \infty$) we use that $\sin^2(\Omega t/2)/(\Omega/2)^2 \approx \pi t \delta(\Omega)$ (here $\delta(\Omega)$ is Dirac's delta function), and therefore the transition probability grows linearly in time. We can find the frictional force equating the frictional work $F_x v$ with the rate of change in time of the energy of the excitations, namely

$$F_x v = \frac{dU}{dt} = \sum_{\mathbf{k}j j'} \hbar(\omega_{u,\mathbf{k}j} + \omega_{l,-\mathbf{k}j'}) \frac{dP_{\mathbf{k}j j'}}{dt}, \quad (26)$$

and the r.h.s. is time-independent since the transition probabilities grow linearly in time. Using the expression (23) for $\beta_{\mathbf{k}j}^2$ and the transition probabilities (25) at large times, and writing the sums over the dielectric degree of freedom j as $\sum_j = \int_0^\infty d\omega dN/d\omega$ (and similarly for j'), one finally obtains the following expression for the frictional force

$$F_x = \frac{\hbar}{\pi} \int \frac{d^2\mathbf{k}}{(2\pi)^2} k_x e^{-2|\mathbf{k}|d} \int_0^{k_x v} d\omega \text{Im} \left[\frac{\varepsilon(\omega) - 1}{\varepsilon(\omega) + 1} \right] \text{Im} \left[\frac{\varepsilon(k_x v - \omega) - 1}{\varepsilon(k_x v - \omega) + 1} \right]. \quad (27)$$

In the literature there are other more rigorous approaches to calculate quantum friction that go beyond the non-retarded quasi-static limit considered above, and that can take into account effects of relativistic motion as well as finite temperature. One of these approaches [73] follows the spirit of the Lifshitz-Rytov theory [74], considering the fluctuating electromagnetic (EM) field as a *classical* field whose stochastic fluctuations satisfy the fluctuation-dissipation relation that relates the field fluctuations with the absorptive part of the dielectric response of the plates. The EM field is a solution to Maxwell's equations with classical fluctuating current densities on the plates as source fields, and it satisfies the usual EM b.c. imposed on the comoving reference frames on each plate. The relation between the EM fields in different frames is obtained via Lorentz transformations. An alternative full quantum-mechanical approach considers the *quantum* EM field in interaction with (quantized) noise polarizations and noise currents within the plates [75]. As before, the fields in each reference frame are related by Lorentz transformations. In this approach the quantum expectation value of the noise currents is given by the (quantum) fluctuation-dissipation relation.

Quantum friction can also happen for neutral atoms moving close to surfaces. The theoretical methods to compute the frictional force in these cases are similar to the surface-surface quantum friction, and we refer the reader to some of the relevant works [76, 77, 78].

4 Resonant photon creation in time dependent cavities

As mentioned in the Introduction, photon creation can be enhanced in closed cavities: if the external time dependence involves a frequency that is twice the frequency of a mode of the electromagnetic field in the (unperturbed) cavity, parametric amplification produces a large number of photons. As we will see, under certain circumstances (ideal three dimensional cavities with non equidistant frequencies in the spectrum) the number of photons in the resonant mode may grow exponentially. Parametric amplification can take place by changing the length of the cavity with a moving surface, but also by changing its effective length through time dependent electromagnetic properties of the cavity.

In order to simplify the notation, in this section we will use the natural units $\hbar = c = 1$.

4.1 Dynamical Casimir effect in 1D cavities

As in Section 2, we start with a massless real scalar field in a 1D cavity with one mirror fixed at $x = 0$ and the other performing an oscillatory motion

$$L(t) = L_0[1 + \varepsilon \sin(\Omega t)], \quad (28)$$

where Ω is the external frequency and $\varepsilon \ll 1$. As we will be mainly concerned with situations where $\Omega L_0 = O(1)$, the maximum velocity of the mirror will be of order ε , and therefore small values of ε correspond to a non-relativistic motion of the mirror. We shall assume that the oscillations begin at $t = 0$, end at $t = T$, and that $L(t) = L_0$ for $t < 0$ and $t > T$. The scalar field $\phi(x, t)$ satisfies the wave equation $\square\phi = 0$ and Dirichlet b.c. $\phi(x = 0, t) = \phi(L(t), t) = 0$. When the mirror is at rest, the eigenfrequencies are multiples of the fundamental frequency π/L_0 . Therefore, in order to analyze resonant situations we will assume that $\Omega = q\pi/L_0$, $q = 1, 2, 3, \dots$

Inside the cavity we can write

$$\phi(x, t) = \sum_{k=1}^{\infty} \left[a_k \psi_k(x, t) + a_k^\dagger \psi_k^*(x, t) \right], \quad (29)$$

where the mode functions $\psi_k(x, t)$ are positive frequency modes for $t < 0$, and a_k and a_k^\dagger are time-independent bosonic annihilation and creation operators, respectively. The field equation is automatically verified by writing the modes in terms of Moore's function $R(t)$ [7] as

$$\psi_k(x, t) = \frac{i}{\sqrt{4\pi k}} \left(e^{-ik\pi R(t+x)} - e^{-ik\pi R(t-x)} \right). \quad (30)$$

The Dirichlet boundary condition is satisfied provided that $R(t)$ satisfies Moore's equation

$$R(t + L(t)) - R(t - L(t)) = 2. \quad (31)$$

These simple expressions for the modes of the field are due to conformal invariance, a symmetry for massless fields in one spatial dimension.

The solution to the problem involves finding a solution $R(t)$ in terms of the prescribed motion $L(t)$. For $t < 0$ the positive frequency modes are given by $R(t) = t/L_0$ for $-L_0 \leq t \leq L_0$, which is indeed a solution to Eq.(31) for $t < 0$. For $t > 0$, Eq.(31) can be solved, for example, using a perturbative expansion in ε similar to the one employed in Section 2 for a single mirror. However, as the external frequency is tuned with the unperturbed modes of the cavity, in general there will be resonant effects, which produce secular terms proportional to $\varepsilon^m (\Omega t)^n$ with $m \leq n$. Thus this expansion is valid only for short times $\varepsilon \Omega t \ll 1$. It is possible to obtain a non-perturbative solution of Eq.(31) using Renormalization Group (RG) techniques [34]. The RG-improved solution automatically adds the most secular terms, $(\varepsilon \Omega t)^n$, to all orders in ε , and is valid for longer times $\varepsilon^2 \Omega t \ll 1$. The RG-improved solution is [34, 79]

$$R(t) = \frac{t}{L_0} - \frac{2}{\pi q} \text{Im} \ln \left[1 + \xi + (1 - \xi) e^{\frac{iq\pi t}{L_0}} \right], \quad (32)$$

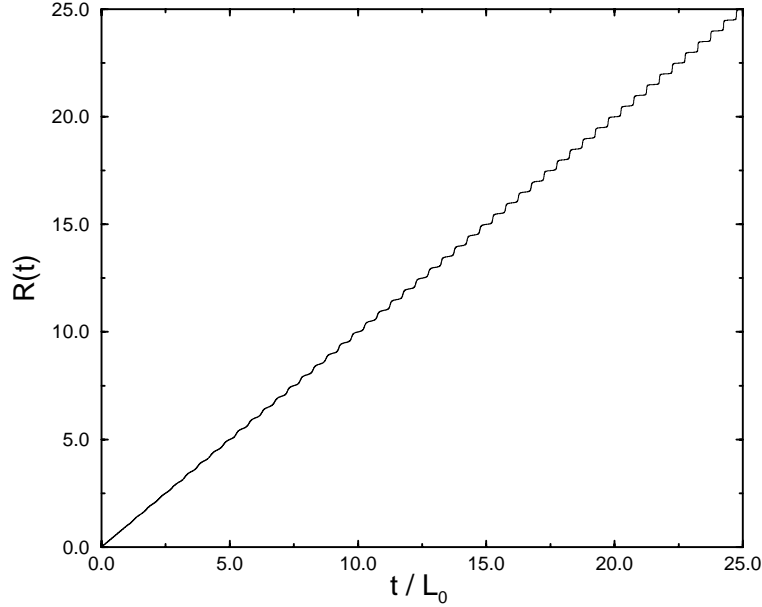


Fig. 2 $R(t)$ vs. t/L_0 as given by Eq.(32). The values of the parameters are $q = 4$ and $\varepsilon = 0.01$.

where $\xi = \exp[(-1)^{q+1}\pi q \varepsilon t/L_0]$. As shown in Fig.2, the function $R(t)$ develops a staircase shape for long times [34, 80]. Within regions of t between odd multiples of L_0 there appear q jumps, located at values of t satisfying $\cos(q\pi t/L_0) = \mp 1$, the upper sign corresponding to even values of q and the lower one to odd values of q .

The vacuum expectation value of the energy density of the field is given by [9] $\langle T_{00}(x,t) \rangle = -f(t+x) - f(t-x)$, where

$$f = \frac{1}{24\pi} \left[\frac{R'''}{R'} - \frac{3}{2} \left(\frac{R''}{R'} \right)^2 + \frac{\pi^2}{2} (R')^2 \right]. \quad (33)$$

For $q = 1$ (“semi-resonant” case) no exponential amplification of the energy density is obtained, whereas for $q \geq 2$ (“resonant” cases) the energy density grows exponentially in the form of q traveling wave packets which become narrower and higher as time increases (see Fig.4). Note that, as the energy density involves the derivatives of the function $R(t)$, there is one peak for each jump of $R(t)$.

The number of created particles can be computed from the solution given by Eq.(32). Photons are created resonantly in all modes with $n = q + 2j$, with j a non-negative integer. This is due to the fact that the spectrum of a one dimensional cavity is *equidistant*: although the external frequency resonates with a particular eigenmode of the cavity, intermode coupling produces resonant creation in the other

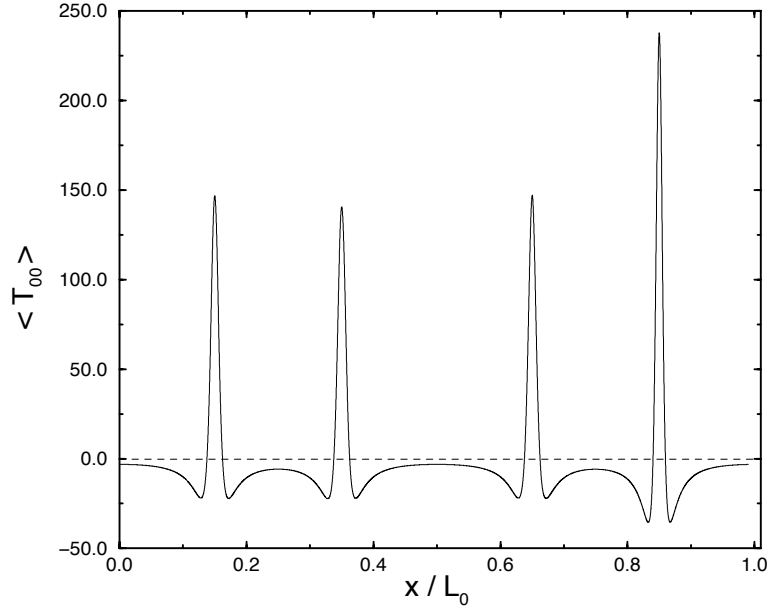


Fig. 3 Energy density profile between plates for fixed time $t/L_0 = 20.4$ for the $q = 4$ case. The amplitude coefficient is $\varepsilon = 0.01$

modes. At long times, the number of photons in each mode grows linearly in time, while the total number of photons grows quadratically and the total energy inside the cavity grows exponentially [30]. These different behaviors are due to the fact that the number of excited modes, i.e. the number of modes that reach a growth linear in time, increases exponentially.

The production of massless particles in one dimensional cavities has been analyzed numerically in Ref. [81]. As expected, the numerical evaluations are in perfect agreement with the analytic results described above in the case of small amplitudes $\varepsilon \leq 0.01$.

The force on the moving mirror can be computed as the discontinuity of $\langle T_{11} \rangle$ at $x = L(t)$. The force produced by the outside field is one -half the expression derived in Section 2. This is much smaller than the intracavity contribution and will be neglected. Therefore

$$\langle F \rangle \approx \langle T_{11}(L(t), t) \rangle = \langle T_{00}(L(t), t) \rangle, \quad (34)$$

where the energy momentum tensor is evaluated *inside* the cavity. This expression reproduces the usual attractive result when the mirror is at rest ($t < 0$)

$$\langle F \rangle = -\frac{\pi}{24L_0^2}, \quad (35)$$

that is, the static Casimir effect in 1D. However, at long times it becomes an exponentially increasing pressure due to the presence of real photons in the cavity [30].

All this treatment can be extended to the case of Neumann b.c. $n^\mu \partial_\mu \phi|_{\text{mirror}} = 0$, where n^μ is a unit two-vector perpendicular to the trajectory of the mirror. The modes of the field can be written in terms of Moore's function $R(t)$ as

$$\phi_k(x, t) = \frac{1}{\sqrt{4\pi k}} \left(e^{-ik\pi R(t+x)} + e^{-ik\pi R(t-x)} \right). \quad (36)$$

Note the change of sign between Eq.(30) for Dirichlet modes, and Eq.(36) for Neumann modes. The spectrum of motion-induced photons is the same for both Dirichlet and Neumann b.c. [60], but not for the mixed configuration with one Dirichlet mirror and one Neumann mirror [82]. The one dimensional DCE has also been investigated for cavities with Robin b.c. [83].

4.2 Photon creation in 3D cavities

The one dimensional DCE with Dirichlet b.c. described in the previous section is not only of academic interest: it describes photon creation for the TEM modes in a 3D cylindrical cavity with a non-simply connected section [33]. However, in order to analyze TE and TM modes in general 3D cavities, a new approach is needed, since conformal invariance is no longer useful in 3D.

We shall first describe in some detail the simpler case of a scalar field in a rectangular cavity satisfying Dirichlet b.c. [31], and then comment on the extension to the case of the electromagnetic field in cylindrical cavities with an arbitrary section.

4.2.1 Scalar field

We consider a rectangular cavity formed by perfectly reflecting walls with dimensions L_x, L_y , and L_z . The wall placed at $z = L_z$ is at rest for $t < 0$ and begins to move following a given trajectory, $L_z(t)$, at $t = 0$. We assume this trajectory as prescribed for the problem (not a dynamical variable) and that it works as a time-dependent boundary condition for the field. The field $\phi(\mathbf{x}, t)$ satisfies the wave equation $\square\phi = 0$, and the b.c. $\phi|_{\text{walls}} = 0$ for all times. The Fourier expansion of the field for an arbitrary moment of time, in terms of creation and annihilation operators, can be written as

$$\phi(\mathbf{x}, t) = \sum_{\mathbf{n}} \hat{a}_{\mathbf{n}}^{\text{in}} u_{\mathbf{n}}(\mathbf{x}, t) + \text{H.c.}, \quad (37)$$

where the mode functions $u_{\mathbf{n}}(\mathbf{x}, t)$ form a complete orthonormal set of solutions of the wave equation with vanishing b.c..

When $t \leq 0$ (static cavity) each field mode is determined by three positive integers n_x, n_y and n_z , namely

$$\begin{aligned} u_{\mathbf{n}}(\mathbf{x}, t < 0) &= \frac{1}{\sqrt{2\omega_{\mathbf{n}}}} \sqrt{\frac{2}{L_x}} \sin\left(\frac{n_x \pi}{L_x} x\right) \sqrt{\frac{2}{L_y}} \sin\left(\frac{n_y \pi}{L_y} y\right) \\ &\times \sqrt{\frac{2}{L_z}} \sin\left(\frac{n_z \pi}{L_z} z\right) e^{-i\omega_{\mathbf{n}} t}, \end{aligned} \quad (38)$$

with $\omega_{\mathbf{n}} = \pi \sqrt{\left(\frac{n_x}{L_x}\right)^2 + \left(\frac{n_y}{L_y}\right)^2 + \left(\frac{n_z}{L_z}\right)^2}$.

When $t > 0$ the boundary condition on the moving wall becomes $\phi(x, y, z = L_z(t), t) = 0$. In order to satisfy it we expand the mode functions in Eq.(37) with respect to an *instantaneous basis* [84]

$$\begin{aligned} u_{\mathbf{n}}(\mathbf{x}, t > 0) &= \sum_{\mathbf{m}} Q_{\mathbf{m}}^{(\mathbf{n})}(t) \sqrt{\frac{2}{L_x}} \sin\left(\frac{m_x \pi}{L_x} x\right) \sqrt{\frac{2}{L_y}} \sin\left(\frac{m_y \pi}{L_y} y\right) \\ &\times \sqrt{\frac{2}{L_z}} \sin\left(\frac{m_z \pi}{L_z(t)} z\right) = \sum_{\mathbf{m}} Q_{\mathbf{m}}^{(\mathbf{n})}(t) \varphi_{\mathbf{m}}(\mathbf{x}, L_z(t)), \end{aligned} \quad (39)$$

with the initial conditions

$$Q_{\mathbf{m}}^{(n)}(0) = \frac{1}{\sqrt{2\omega_{\mathbf{n}}}} \delta_{\mathbf{m},\mathbf{n}}, \quad \dot{Q}_{\mathbf{m}}^{(n)}(0) = -i\sqrt{\frac{\omega_{\mathbf{n}}}{2}} \delta_{\mathbf{m},\mathbf{n}}. \quad (40)$$

In this way we ensure that, as long as $L_z(t)$ and $\dot{L}_z(t)$ are continuous at $t = 0$, each field mode and its time derivative are also continuous functions. The expansion in Eq.(39) for the field modes must be a solution of the wave equation. Taking into account that the $\varphi_{\mathbf{k}}$'s form a complete and orthonormal set and that they depend on t only through $L_z(t)$, we obtain a set of (exact) coupled equations for $Q_{\mathbf{m}}^{(n)}(t)$ [31]:

$$\begin{aligned} \ddot{Q}_{\mathbf{m}}^{(n)} + \omega_{\mathbf{m}}^2(t) Q_{\mathbf{m}}^{(n)} &= 2\lambda(t) \sum_{\mathbf{j}} g_{\mathbf{mj}} \dot{Q}_{\mathbf{j}}^{(n)} + \dot{\lambda}(t) \sum_{\mathbf{j}} g_{\mathbf{mj}} Q_{\mathbf{j}}^{(n)} \\ &+ \lambda^2(t) \sum_{\mathbf{j},\mathbf{l}} g_{\mathbf{lm}} g_{\mathbf{l}\mathbf{j}} Q_{\mathbf{j}}^{(n)}, \end{aligned} \quad (41)$$

where

$$\omega_{\mathbf{m}}(t) = \pi \sqrt{\left(\frac{m_x}{L_x}\right)^2 + \left(\frac{m_y}{L_y}\right)^2 + \left(\frac{m_z}{L_z(t)}\right)^2}; \quad \lambda(t) = \frac{\dot{L}_z(t)}{L_z(t)}. \quad (42)$$

The coefficients $g_{\mathbf{mj}}$ are defined by

$$g_{\mathbf{mj}} = -g_{\mathbf{jm}} = L_z(t) \int_0^{L_z(t)} dz \frac{\partial \varphi_{\mathbf{m}}}{\partial L_z} \varphi_{\mathbf{j}}. \quad (43)$$

The annihilation and creation operators $\hat{a}_{\mathbf{m}}^{\text{in}}$ and $\hat{a}_{\mathbf{m}}^{\dagger\text{in}}$ correspond to the particle notion in the 'in' region ($t < 0$). If the wall stops for $t > t_{\text{final}}$, we can define a new set of operators, $\hat{a}_{\mathbf{m}}^{\text{out}}$ and $\hat{a}_{\mathbf{m}}^{\dagger\text{out}}$, associated with the particle notion in the 'out' region ($t > t_{\text{final}}$). These two sets of operators are connected by means of the Bogoliubov transformation

$$\hat{a}_{\mathbf{m}}^{\text{out}} = \sum_{\mathbf{n}} (\hat{a}_{\mathbf{n}}^{\text{in}} \alpha_{\mathbf{nm}} + \hat{a}_{\mathbf{n}}^{\dagger\text{in}} \beta_{\mathbf{nm}}^*). \quad (44)$$

The coefficients $\alpha_{\mathbf{nm}}$ and $\beta_{\mathbf{nm}}$ can be obtained as follows. When the wall returns to its initial position the right hand side in Eq.(41) vanishes and the solution is

$$Q_{\mathbf{m}}^{(n)}(t > t_{\text{final}}) = A_{\mathbf{m}}^{(n)} e^{i\omega_{\mathbf{m}}t} + B_{\mathbf{m}}^{(n)} e^{-i\omega_{\mathbf{m}}t}, \quad (45)$$

with $A_{\mathbf{m}}^{(n)}$ and $B_{\mathbf{m}}^{(n)}$ being some constant coefficients to be determined by the continuity conditions at $t = t_{\text{final}}$. Inserting Eq.(45) into Eqs.(37) and (39) we obtain an expansion of ϕ in terms of $\hat{a}_{\mathbf{m}}^{\text{in}}$ and $\hat{a}_{\mathbf{m}}^{\dagger\text{in}}$ for $t > t_{\text{final}}$. Comparing this with the equivalent expansion in terms of $\hat{a}_{\mathbf{m}}^{\text{out}}$ and $\hat{a}_{\mathbf{m}}^{\dagger\text{out}}$ it is easy to see that

$$\alpha_{\mathbf{nm}} = \sqrt{2\omega_{\mathbf{m}}B_{\mathbf{m}}^{(n)}}, \quad \beta_{\mathbf{nm}} = \sqrt{2\omega_{\mathbf{m}}A_{\mathbf{m}}^{(n)}}. \quad (46)$$

The amount of photons created in the mode \mathbf{m} is the average value of the number operator $\hat{a}_{\mathbf{m}}^{\dagger\text{out}} \hat{a}_{\mathbf{m}}^{\text{out}}$ with respect to the initial vacuum state (defined through $\hat{a}_{\mathbf{m}}^{\text{in}}|0_{\text{in}}\rangle =$

0). With the help of Eq.(44) and Eq.(46) we find

$$\langle \mathcal{N}_{\mathbf{m}} \rangle = \langle 0_{\text{in}} | \hat{a}_{\mathbf{m}}^{\dagger \text{out}} \hat{a}_{\mathbf{m}}^{\text{out}} | 0_{\text{in}} \rangle = \sum_{\mathbf{n}} 2\omega_{\mathbf{m}} |A_{\mathbf{m}}^{(\mathbf{n})}|^2. \quad (47)$$

In the approach described so far we worked at the level of the dynamical equation for the quantum scalar field. Alternatively, one can analyze the problem using the *effective Hamiltonian method* developed in Ref. [85]. The idea is the following. Assume that a massless scalar field is confined within a time dependent volume and satisfies Dirichlet b.c.. At the classical level, the field can be expanded in terms of a basis of functions $f_{\alpha}(\mathbf{x}, t)$ that fulfill the b.c. at each time, that is

$$\phi(\mathbf{x}, t) = \sum_{\alpha} q_{\alpha}(t) f_{\alpha}(\mathbf{x}, t). \quad (48)$$

For the rectangular cavities considered in this section these functions can be chosen to be $\varphi_{\mathbf{m}}(\mathbf{x}, L_z(t))$. Inserting this expansion into the Klein-Gordon Lagrangian, one ends up with a Lagrangian for the generalized coordinates $q_{\alpha}(t)$, which is a quadratic function of $q_{\alpha}(t)$ and $\dot{q}_{\alpha}(t)$, i.e. it describes a set of coupled harmonic oscillators with time dependent frequencies and couplings. This system can be quantized following the usual procedure, and the final results for the number of created photons are equivalent to those obtained in Eq. (47).

4.2.2 Parametric amplification in 3D

As in Section 4.1, we are interested in resonant situations where the number of photons created inside the cavity could be enhanced for some specific external frequencies. So we study the trajectory given in Eq.(28). To first order in ε , the equations for the modes Eq.(41) take the form

$$\begin{aligned} \ddot{Q}_{\mathbf{m}}^{(\mathbf{n})} + \omega_{\mathbf{m}}^2 Q_{\mathbf{m}}^{(\mathbf{n})} &= 2\varepsilon \left(\frac{\pi m_z}{L_z} \right)^2 \sin(\Omega t) Q_{\mathbf{m}}^{(\mathbf{n})} - \varepsilon \Omega^2 \sin(\Omega t) \sum_{\mathbf{j}} g_{\mathbf{mj}} Q_{\mathbf{j}}^{(\mathbf{n})} \\ &+ 2\varepsilon \Omega \cos(\Omega t) \sum_{\mathbf{j}} g_{\mathbf{mj}} \dot{Q}_{\mathbf{j}}^{(\mathbf{n})} + O(\varepsilon^2). \end{aligned} \quad (49)$$

It is known that a naive perturbative solution of these equations in powers of the displacement ε breaks down after a short amount of time, of order $(\varepsilon \Omega)^{-1}$. As in the 1D case discussed in the previous section, this happens for those particular values of the external frequency Ω such that there is a resonant coupling with the eigenfrequencies of the static cavity. In this situation, to find a solution valid for longer times (of order $\varepsilon^{-2} \Omega^{-1}$) we proceed as follows. We assume that the solution of Eq.(49) is of the form

$$Q_{\mathbf{m}}^{(\mathbf{n})}(t) = A_{\mathbf{m}}^{(\mathbf{n})}(t) e^{i\omega_{\mathbf{m}} t} + B_{\mathbf{m}}^{(\mathbf{n})}(t) e^{-i\omega_{\mathbf{m}} t}, \quad (50)$$

where the functions $A_{\mathbf{m}}^{(n)}$ and $B_{\mathbf{m}}^{(n)}$ are slowly varying. In order to obtain differential equations for them, we insert this ansatz into Eq.(49) and neglect second-order derivatives of $A_{\mathbf{m}}^{(n)}$ and $B_{\mathbf{m}}^{(n)}$. After multiplying the equation by $e^{\pm i\omega_{\mathbf{m}}t}$ we average over the fast oscillations. The resulting equations are

$$\begin{aligned} \frac{1}{\varepsilon} \frac{dA_{\mathbf{m}}^{(n)}}{dt} &= -\frac{\pi^2 m_z^2}{2\omega_{\mathbf{m}} L_z^2} B_{\mathbf{m}}^{(n)} \delta(2\omega_{\mathbf{m}} - \Omega) \\ &+ \sum_{\mathbf{j}} \left(-\omega_{\mathbf{j}} + \frac{\Omega}{2}\right) \delta(-\omega_{\mathbf{m}} - \omega_{\mathbf{j}} + \Omega) \frac{\Omega}{2\omega_{\mathbf{m}}} g_{\mathbf{kj}} B_{\mathbf{j}}^{(n)} \\ &+ \sum_{\mathbf{j}} \left[\left(\omega_{\mathbf{j}} + \frac{\Omega}{2}\right) \delta(\omega_{\mathbf{m}} - \omega_{\mathbf{j}} - \Omega) + \left(\omega_{\mathbf{j}} - \frac{\Omega}{2}\right) \delta(\omega_{\mathbf{m}} - \omega_{\mathbf{j}} + \Omega) \right] \\ &\times \frac{\Omega}{2\omega_{\mathbf{m}}} g_{\mathbf{mj}} A_{\mathbf{j}}^{(n)}, \end{aligned} \quad (51)$$

and

$$\begin{aligned} \frac{1}{\varepsilon} \frac{dB_{\mathbf{m}}^{(n)}}{dt} &= -\frac{\pi^2 m_z^2}{2\omega_{\mathbf{m}} L_z^2} A_{\mathbf{m}}^{(n)} \delta(2\omega_{\mathbf{m}} - \Omega) \\ &+ \sum_{\mathbf{j}} \left(-\omega_{\mathbf{j}} + \frac{\Omega}{2}\right) \delta(-\omega_{\mathbf{m}} - \omega_{\mathbf{j}} + \Omega) \frac{\Omega}{2\omega_{\mathbf{m}}} g_{\mathbf{mj}} A_{\mathbf{j}}^{(n)} \\ &+ \sum_{\mathbf{j}} \left[\left(\omega_{\mathbf{j}} + \frac{\Omega}{2}\right) \delta(\omega_{\mathbf{m}} - \omega_{\mathbf{j}} - \Omega) + \left(\omega_{\mathbf{j}} - \frac{\Omega}{2}\right) \delta(\omega_{\mathbf{m}} - \omega_{\mathbf{j}} + \Omega) \right] \\ &\times \frac{\Omega}{2\omega_{\mathbf{m}}} g_{\mathbf{mj}} B_{\mathbf{j}}^{(n)}, \end{aligned} \quad (52)$$

where we used the notation $\delta(\omega)$ for the Kronecker δ -function $\delta_{\omega 0}$.

The method used to derive these equations is equivalent to the ‘‘multiple scale analysis’’ [86] and to the slowly varying envelope approximation [87]. The equations are non-trivial (i.e., lead to resonant behavior) if $\Omega = 2\omega_{\mathbf{m}}$ (resonant condition). Moreover, there is intermode coupling between modes \mathbf{j} and \mathbf{m} if any of the conditions $|\omega_{\mathbf{m}} \pm \omega_{\mathbf{j}}| = \Omega$ is satisfied.

We derived the equations for three dimensional cavities. It is easy to obtain the corresponding ones for one dimensional cavities. The conditions for resonance and intermode coupling are the same. The main difference is that for one dimensional cavities the spectrum is equidistant. Therefore an infinite set of modes may be coupled. For example, when the external frequency is $\Omega = 2\omega_1$, the mode m is coupled with the modes $m \pm 2$. This has been extensively studied in the literature [34, 30, 88, 89].

In what follows we will be concerned with cavities with non-equidistant spectrum. Eqs.(51) and (52) present different kinds of solutions depending both on the mirror’s frequency and the spectrum of the static cavity. In the simplest ‘parametric resonance case’ the frequency of the mirror is twice the frequency of some unper-

turbed mode, say $\Omega = 2\omega_{\mathbf{m}}$. In order to find $A_{\mathbf{m}}^{(n)}$ and $B_{\mathbf{m}}^{(n)}$ from Eq.(51) and Eq.(52) we have to analyze whether the coupling conditions $|\omega_{\mathbf{m}} \pm \omega_{\mathbf{j}}| = \Omega$ can be satisfied or not. If we set $\Omega = 2\omega_{\mathbf{m}}$, the resonant mode \mathbf{m} will be coupled to some other mode \mathbf{j} only if $\omega_{\mathbf{j}} - \omega_{\mathbf{m}} = \Omega = 2\omega_{\mathbf{m}}$. Clearly, the latter relation will be satisfied depending on the spectrum of the particular cavity under consideration.

Let us assume that this condition is not fulfilled. In this case, the equations for $A_{\mathbf{m}}^{(n)}$ and $B_{\mathbf{m}}^{(n)}$ can be easily solved and give

$$\langle \mathcal{N}_{\mathbf{m}} \rangle = \sinh^2 \left[\frac{1}{\Omega} \left(\frac{m_z \pi}{L_z} \right)^2 \varepsilon t_f \right]. \quad (53)$$

In this uncoupled resonance case the average number of created photons in the mode \mathbf{m} increases exponentially in time. Another way of looking at this particular situation is to note that, neglecting the intermode couplings, the amplitude of the resonant mode satisfies the equation of an harmonic oscillator with time dependent frequency. For the particular trajectory given in Eq.(28), the dynamics of the mode is governed by Eq. (49) with $g_{\mathbf{mj}} = 0$, that is

$$\ddot{Q}_{\mathbf{m}}^{(n)} + \left[\omega_{\mathbf{m}}^2 - 2\varepsilon \left(\frac{\pi m_z}{L_z} \right)^2 \sin(\Omega t) \right] Q_{\mathbf{m}}^{(n)} = 0, \quad (54)$$

which is the well known Mathieu equation [86]. The solutions to this equation have an exponentially growing amplitude when $\Omega = 2\omega_{\mathbf{m}}$.

There are simple situations in which there is intermode coupling. For instance for a cubic cavity of size L , the fundamental mode $(1, 1, 1)$ is coupled to the mode $(5, 1, 1)$ when the external frequency is $\Omega = 2\omega_{111}$. In this case the number of photons in each mode grows with a lower rate than that of the uncoupled case [31]

$$\langle \mathcal{N}_{111} \rangle \simeq \langle \mathcal{N}_{511} \rangle \simeq e^{0.9\varepsilon t_f/L}. \quad (55)$$

We will describe some additional examples of intermode coupling in the next subsection, in the context of a full electromagnetic model.

It is worth stressing that the creation of scalar particles in 3D cavities has been studied numerically in Ref.[90]. At long times, the numerical results coincide with the analytical predictions derived from Eqs.(51) and (52), both in the presence and absence of intermode coupling.

4.2.3 The electromagnetic case

The previous results have been generalized to the case of the electromagnetic field inside a cylindrical cavity, with an arbitrary transversal section [33]. Let us assume that the axis of the cavity is along the z -direction, and that the caps are located at $z = 0$ and $z = L_z(t)$. All the surfaces are perfect conductors.

When studying the electromagnetic field inside these cavities it is convenient to express the physical degrees of freedom in terms of the vector potentials $\mathbf{A}^{(\text{TE})}$ and $\mathcal{A}^{(\text{TM})}$ introduced in Section 2. These vectors can be written in terms of the so called ‘‘scalar Hertz potentials’’ as $\mathbf{A}^{(\text{TE})} = \hat{\mathbf{z}} \times \nabla \phi^{\text{TE}}$ and $\mathcal{A}^{(\text{TM})} = \hat{\mathbf{z}} \times \nabla \phi^{\text{TM}}$. For perfect reflectors the b.c. do not mix TE and TM polarizations, and therefore the electromagnetic field inside the cavity can be described in terms of these two *independent* scalar Hertz potentials: no crossed terms appear in Maxwell’s Lagrangian or Hamiltonian.

The scalar Hertz potentials satisfy the Klein-Gordon equation. The b.c. of both potentials on the static walls of the cavity are

$$\phi^{\text{TE}}|_{z=0} = 0 ; \frac{\partial \phi^{\text{TE}}}{\partial n}|_{\text{trans}} = 0, \quad (56)$$

$$\frac{\partial \phi^{\text{TM}}}{\partial z}|_{z=0} = 0 ; \phi^{\text{TM}}|_{\text{trans}} = 0, \quad (57)$$

where $\partial/\partial n$ denotes the normal derivative on the transverse boundaries. On the other hand, the b.c. on the moving mirror has been already discussed in Section 2 (see Eqs (16) and (17)). In terms of the Hertz potentials they read as

$$\phi^{\text{TE}}|_{z=L_z(t)} = 0 ; (\partial_z + \dot{L}_z \partial_t) \phi^{\text{TM}}|_{L_z(t)} = 0. \quad (58)$$

The energy of the electromagnetic field

$$H = \frac{1}{8\pi} \int d^3x (\mathbf{E}^2 + \mathbf{B}^2) = H^{\text{TE}} + H^{\text{TM}} \quad (59)$$

can be written in terms of the scalar potentials as

$$H^{(\text{P})} = \frac{1}{8\pi} \int d^3x \left[\dot{\phi}^{(\text{P})} (-\nabla_{\perp}^2) \dot{\phi}^{(\text{P})} + \phi^{(\text{P})'} (-\nabla_{\perp}^2) \phi^{(\text{P})'} + \nabla_{\perp}^2 \phi^{(\text{P})} \nabla_{\perp}^2 \phi^{(\text{P})} \right], \quad (60)$$

where dots and primes denote derivatives with respect to time and z respectively. The supraindex P corresponds to TE and TM and ∇_{\perp} denotes the gradient on the xy plane.

The quantization procedure has been described in detail in previous papers [32, 33, 91]. At any given time both scalar Hertz potentials can be expanded in terms of an instantaneous basis

$$\phi^{(\text{P})}(\mathbf{x}, t) = \sum_{\mathbf{n}} a_{\mathbf{n}}^{\text{IN}} C_{\mathbf{n}}^{(\text{P})} u_{\mathbf{n}}^{(\text{P})}(\mathbf{x}, t) + \text{c.c.}, \quad (61)$$

where $a_{\mathbf{n}}^{\text{IN}}$ are bosonic operators that annihilate the IN vacuum state for $t < 0$, and $C_{\mathbf{n}}^{(\text{P})}$ are normalization constants that must be appropriately included to obtain the usual form of the electromagnetic Hamiltonian (60) in terms of annihilation and creation operators.

For TE modes, the mode functions are similar to those of the scalar field satisfying Dirichlet b.c. described in the previous section

$$u_{\mathbf{n}}^{\text{TE}} = \sum_{\mathbf{m}} Q_{\mathbf{m},\text{TE}}^{(\mathbf{n})}(t) \sqrt{2/L_z(t)} \sin\left(\frac{m_z \pi z}{L_z(t)}\right) v_{\mathbf{m}_{\perp}}(\mathbf{x}_{\perp}). \quad (62)$$

For TM modes, the choice of the instantaneous basis is less trivial and has been derived in detail in Ref. [32]

$$u_{\mathbf{n}}^{\text{TM}} = \sum_{\mathbf{m}} [Q_{\mathbf{m},\text{TM}}^{(\mathbf{n})}(t) + \dot{Q}_{\mathbf{m},\text{TM}}^{(\mathbf{n})}(t) g(z,t)] \sqrt{2/L_z(t)} \cos\left(\frac{m_z \pi z}{L_z(t)}\right) r_{\mathbf{m}_{\perp}}(\mathbf{x}_{\perp}). \quad (63)$$

Here the index $\mathbf{m} \neq 0$ is a vector of non-negative integers. The function $g(z,t) = \dot{L}_z(t)L_z(t)\xi(z/L_z(t))$ (where $\xi(z)$ is a solution to the conditions $\xi(0) = \xi(1) = \partial_z \xi(0) = 0$, and $\partial_z \xi(1) = -1$) appears when expanding the TM modes in an instantaneous basis and taking the small ε limit. There are many solutions for $\xi(z)$, but all of them can be shown to lead to the same physical results [32]. The mode functions $v_{\mathbf{m}_{\perp}}(\mathbf{x}_{\perp})$ and $r_{\mathbf{m}_{\perp}}(\mathbf{x}_{\perp})$, are described below for different types of cavities.

The mode functions $Q_{\mathbf{m},\text{TE/TM}}^{(\mathbf{n})}$ satisfy second order, mode-coupled linear differential equations similar to Eq. (49) [32]. As before, for the ‘‘parametric resonant case’’ ($\Omega = 2\omega_{\mathbf{n}}$ for some \mathbf{n}) there is parametric amplification. Moreover, for some particular geometries and sizes of the cavities, different modes \mathbf{n} and \mathbf{m} can be coupled, provided either of the resonant coupling conditions $\Omega = |\omega_{\mathbf{n}} \pm \omega_{\mathbf{m}}|$ are met. When intermode coupling occurs it affects the rate of photon creation, typically resulting in a reduction of that rate.

The number of motion-induced photons with a given wavevector \mathbf{n} and polarization TE or TM can be calculated in terms of the Bogoliubov coefficients. When the resonant coupling conditions are not met, the different modes will not be coupled during the dynamics. As in the scalar case, the system can be described by a Mathieu equation (54) for a single mode. As a consequence, the number of motion-induced photons in that given mode will grow exponentially. The growth rate is different for TE and TM modes [32]

$$\langle \mathcal{N}_{\mathbf{n},\text{TE}}(t) \rangle = \sinh^2(\lambda_{\mathbf{n},\text{TE}} \varepsilon t) ; \quad \langle \mathcal{N}_{\mathbf{n},\text{TM}}(t) \rangle = \sinh^2(\lambda_{\mathbf{n},\text{TM}} \varepsilon t), \quad (64)$$

where $\lambda_{\mathbf{n},\text{TE}} = n_z^2/2\omega_{\mathbf{n}}$ and $\lambda_{\mathbf{n},\text{TM}} = (2\omega_{\mathbf{n}}^2 - n_z^2)/2\omega_{\mathbf{n}}$. When both polarizations are present, the rate of growth for TM photons is larger than for TE photons, *i.e.*, $\lambda_{\mathbf{n},\text{TM}} > \lambda_{\mathbf{n},\text{TE}}$. As in the case of the scalar field, these equations are valid for $\varepsilon^2 \Omega t \ll 1$.

We describe some specific examples:

Rectangular section. For a waveguide of length $L_z(t)$ and transversal rectangular shape (lengths L_x, L_y), the TE mode function is

$$v_{n_x, n_y}(\mathbf{x}_{\perp}) = \frac{2}{\sqrt{L_x L_y}} \cos\left(\frac{n_x \pi x}{L_x}\right) \cos\left(\frac{n_y \pi y}{L_y}\right), \quad (65)$$

with n_x and n_y non-negative integers that cannot be simultaneously zero. The spectrum is

$$\omega_{n_x, n_y, n_z} = \sqrt{(n_x \pi / L_x)^2 + (n_y \pi / L_y)^2 + (n_z \pi / L_z)^2}, \quad (66)$$

with $n_z \geq 1$. The TM mode function is

$$r_{m_x, m_y}(\mathbf{x}_\perp) = \frac{2}{\sqrt{L_x L_y}} \sin\left(\frac{m_x \pi x}{L_x}\right) \sin\left(\frac{m_y \pi y}{L_y}\right), \quad (67)$$

where m_x, m_y are positive integers. The spectrum is given by ω_{m_x, m_y, m_z} , with $m_z \geq 0$.

Let us analyze the particular case of a cubic cavity of size L under the parametric resonant condition $\Omega = 2\omega_{\mathbf{k}}$. The fundamental TE mode is doubly degenerate $((1, 0, 1)$ and $(0, 1, 1))$ and uncoupled to other modes. The number of photons in these TE modes grows as $\exp(\pi \epsilon t \sqrt{2} L)$. The fundamental TM mode $(1, 1, 0)$ has the same energy as the fundamental TE mode, and it is coupled to the TM mode $(1, 1, 4)$. Motion-induced TM photons are produced exponentially as $\exp(4.4 \epsilon t / L)$, much faster than TE photons.

Circular section. For a waveguide with a transversal circular shape of radius R , the TE mode function is

$$v_{nm}(\mathbf{x}_\perp) = \frac{1}{\sqrt{\pi}} \frac{1}{R J_n(y_{nm}) \sqrt{1 - n^2 / y_{nm}^2}} J_n\left(y_{nm} \frac{\rho}{R}\right) e^{in\phi}, \quad (68)$$

where J_n denotes the Bessel function of n th order, and y_{nm} is the m th positive root of the equation $J'_n(y) = 0$. The eigenfrequencies are given by

$$\omega_{n, m, n_z} = \sqrt{\left(\frac{y_{nm}}{R}\right)^2 + \left(\frac{n_z \pi}{L_z}\right)^2}, \quad (69)$$

where $n_z \geq 1$. The TM mode function is

$$r_{nm}(\mathbf{x}_\perp) = \frac{1}{\sqrt{\pi}} \frac{1}{R J_{n+1}(x_{nm})} J_n\left(x_{nm} \frac{\rho}{R}\right) e^{in\phi}, \quad (70)$$

where x_{nm} is the m th root of the equation $J_n(x) = 0$. The spectrum is given by Eq.(69) with y_{nm} replaced by x_{nm} and $n_z \geq 0$. Denoting the modes by (n, m, n_z) , the lowest TE mode is $(1, 1, 1)$ and has a frequency $\omega_{111} = (1.841/R) \sqrt{1 + 2.912(R/L_z)^2}$. This mode is uncoupled to any other modes, and the number of photons in this mode grows exponentially in time as $\exp(\pi \epsilon t / \sqrt{1 + 0.343(L_z/R)^2 L_z})$ when parametrically excited. The lowest TM mode $(0, 1, 0)$ is also uncoupled and has a frequency $\omega_{010} = 2.405/R$. The parametric growth is $\exp(4.81 \epsilon t / R)$. For L_z large enough ($L_z > 2.03R$), the resonance frequency ω_{111} of the lowest TE mode is smaller than that for the lowest TM mode. Then the $(1, 1, 1)$ TE mode is the fundamental oscillation of the cavity.

4.3 Time dependent electromagnetic properties

From a theoretical point of view, it is possible to create photons from the vacuum not only for a cavity with a moving mirror, but also when the electromagnetic properties of the walls and/or the media inside the cavity change with time. Given the difficulties in a possible experimental verification of the DCE for moving mirrors, the consideration of time dependent properties is not only of academic interest, but it is also relevant for the analysis of the experimental proposals discussed in Section 5.

A setup that has attracted both theoretical and experimental attention is the possibility of using short laser pulses in order to produce periodic variations of the conductivity of a semiconductor layer placed inside a microwave cavity. The fast changes in the conductivity induce a periodic variation in the effective length of the cavity, and therefore the creation of photon pairs [42, 43]. This setup has been analyzed at the theoretical level [44, 92, 93, 94], and there is an ongoing experiment aimed at the detection of the motion induced radiation [46] (see Section 5).

For the sake of clarity we discuss in detail the model of a massless scalar field within a rectangular cavity with perfect conducting walls with dimensions L_x , L_y , and L_z described in Ref.[44]. At the midpoint of the cavity ($x = L_x/2$) there is a plasma sheet. We model the conductivity properties of such material by a delta-potential with a time dependent strength $V(t)$. This is a time dependent generalization of the model introduced in Ref.[66]. The strength of the potential is given by

$$V(t) = 4\pi \frac{e^2 n(t)}{m^*}, \quad (71)$$

where e is the electron charge, m^* the electron's effective mass in the conduction band and $n(t)$ the surface density of carriers. We assume that the irradiation of the plasma sheet produces changes in this quantity. The ideal limit of perfect conductivity corresponds to $V \rightarrow \infty$, and $V \rightarrow 0$ to a 'transparent' material. The strength of the potential varies between a minimum value, V_0 , and a maximum V_{\max} . The Lagrangian of the scalar field within the cavity is given by

$$\mathcal{L} = \frac{1}{2} \partial_\mu \phi \partial^\mu \phi - \frac{V(t)}{2} \delta(x - L_x/2) \phi^2, \quad (72)$$

where $\delta(x)$ is the one-dimensional Dirac delta function. The use of an infinitely thin film is justified as long as the width of the slab is much smaller than the wavelengths of the relevant electromagnetic modes in the cavity. The corresponding Lagrange equation reads,

$$(\nabla^2 - \partial_t^2) \phi = V(t) \delta(x - L_x/2) \phi. \quad (73)$$

We divide the cavity into two regions: region I ($0 \leq x \leq L_x/2$) and region II ($L_x/2 \leq x \leq L_x$). Perfect conductivity at the edges of the cavity imposes Dirichlet b.c. for the field. The presence of the plasma sheet introduces a discontinuity in the x -spatial derivative, while the field itself remains continuous,

$$\begin{aligned}\phi_I(x = L_x/2, t) &= \phi_{II}(x = L_x/2, t), \\ \partial_x \phi_I(x = L_x/2, t) - \partial_x \phi_{II}(x = L_x/2, t) &= -V(t)\phi(x = L_x/2, t).\end{aligned}\quad (74)$$

We will consider a set of solutions that satisfies automatically all b.c..

$$\psi_{\mathbf{m}}(\mathbf{x}, t) = \sqrt{\frac{2}{L_x}} \sin(k_{m_x}(t)x) \sqrt{\frac{2}{L_y}} \sin\left(\frac{\pi m_y y}{L_y}\right) \sqrt{\frac{2}{L_z}} \sin\left(\frac{\pi m_z z}{L_z}\right), \quad (75)$$

where m_y, m_z are positive integers. The function $\psi_{\mathbf{m}}$ depends on t through $k_{m_x}(t)$, which is the m_x -th positive solution to the following transcendental equation

$$2k_{m_x} \tan^{-1}\left(\frac{k_{m_x} L_x}{2}\right) = -V(t). \quad (76)$$

To simplify the notation, in what follows we will write k_m instead of k_{m_x} . Note that, when $V(t) \rightarrow \infty$, the solutions to this equation become the usual ones for perfect reflectors, $k_m = m L_x/2$, with m a positive integer.

Let us define

$$\Psi_{\mathbf{m}}(\mathbf{x}, t) = \begin{cases} \psi_{\mathbf{m}}(x, y, z, t) & 0 \leq x \leq L_x/2 \\ -\psi_{\mathbf{m}}(x - L_x, y, z, t) & L_x/2 \leq x \leq L_x \end{cases} \quad (77)$$

These functions satisfy the b.c. and the orthogonality relations

$$(\Psi_{\mathbf{m}}, \Psi_{\mathbf{n}}) = [1 - \sin(k_m(t)L_x)/k_m(t)L_x] \delta_{\mathbf{m}, \mathbf{n}}.$$

There is a second set of modes with a node on the cavity midpoint. As these solutions do not “see” the slab, they will be irrelevant in what follows.

For $t \leq 0$ the slab is not irradiated, consequently V is independent of time and has the value V_0 . The modes of the quantum scalar field that satisfy the Klein Gordon equation (73) are

$$u_{\mathbf{m}}(\mathbf{x}, t) = \frac{e^{-i\bar{\omega}_{\mathbf{m}}t}}{\sqrt{2\bar{\omega}_{\mathbf{m}}}} \Psi_{\mathbf{m}}(\mathbf{x}, 0), \quad (78)$$

where $\bar{\omega}_{\mathbf{m}}^2 = (k_m^0)^2 + \left(\frac{\pi m_y}{L_y}\right)^2 + \left(\frac{\pi m_z}{L_z}\right)^2$ and k_m^0 is the m -th solution to Eq.(76) for $V = V_0$. At $t = 0$ the potential starts to change in time and the set of numbers $\{k_m\}$ acquires a time dependence through Eq.(76).

Using Eq. (78) we expand the field operator ϕ as

$$\phi(\mathbf{x}, t) = \sum_{\mathbf{m}} [b_{\mathbf{m}} u_{\mathbf{m}}(\mathbf{x}, t) + b_{\mathbf{m}}^\dagger u_{\mathbf{m}}^*(\mathbf{x}, t)], \quad (79)$$

where $b_{\mathbf{m}}$ are annihilation operators. Notice that in the above equation we omitted the modes with a node at $x = L_x/2$ because their dynamics is not affected by the presence of the slab.

For $t \geq 0$ we write the expansion of the field mode $u_{\mathbf{s}}$ as

$$u_s(\mathbf{x}, t > 0) = \sum_{\mathbf{m}} P_{\mathbf{m}}^{(s)}(t) \Psi_{\mathbf{m}}(\mathbf{x}, t). \quad (80)$$

Assume a time dependent conductivity given by

$$V(t) = V_0 + (V_{\max} - V_0) f(t), \quad (81)$$

where $f(t)$ is a periodic and non-negative function, $f(t) = f(t + T) \geq 0$, that vanishes at $t = 0$ and attains its maximum at $f(\tau_e) = 1$. In each period, $f(t)$ describes the excitation and relaxation of the plasma sheet produced by the laser pulse. Typically, the characteristic time of excitation τ_e is the smallest time scale and satisfies $\tau_e \ll T$. Under certain constraints, large changes in V induce only small variations in k through the transcendental relation between k and V (see Eq. (76)). In this case, a perturbative treatment is valid and a linearization of such a relation is appropriate. Accordingly we write

$$k_n(t) = k_n^0(1 + \varepsilon_n f(t)), \quad (82)$$

where

$$\varepsilon_n = \frac{V_{\max} - V_0}{L_x (k_n^0)^2 + V_0 \left(1 + \frac{V_0 L_x}{4}\right)}. \quad (83)$$

The restriction for the validity of the perturbative treatment is $V_0 L_x \gg V_{\max}/V_0 > 1$. These conditions are satisfied for realistic values of L_x , V_0 , and V_{\max} .

Replacing Eq.(80) into $(\nabla^2 - \partial_t^2)u_s = 0$ we find a set of coupled differential equations for the amplitudes $P_{\mathbf{m}}^{(s)}(t)$. The dynamics is described by a set of coupled harmonic oscillators with periodic frequencies and couplings, as already discussed in this section. It is of the same form as the equations that describe the modes of a scalar field in a three dimensional cavity with an oscillating boundary. For the same reasons as before, a naive perturbative solution of previous equations in powers of ε_n breaks down after a short amount of time when the external frequency is tuned with some of the eigenfrequencies of the cavity. Assuming that $f(t)$ is a sum of harmonic functions of frequencies $\Omega_j = j2\pi/T$, the resonance condition is $\Omega_j = 2\tilde{\omega}_{\mathbf{n}}$ for some j and \mathbf{n} . If there is no intermode coupling, a nonperturbative solution gives an exponential number of created photons in that particular mode

$$\langle \mathcal{N}_{\mathbf{n}}(t) \rangle = \langle b_{\mathbf{n}}^\dagger b_{\mathbf{n}} \rangle = \sum_{\mathbf{s}} 2\tilde{\omega}_{\mathbf{n}} |A_{\mathbf{n}}^{(\mathbf{s})}(t)|^2 \approx \sinh^2 \left(\frac{(k_n^0)^2 f_j}{\Omega_j} \varepsilon_n t \right), \quad (84)$$

where f_j is the amplitude of the oscillations of $f(t)$ with frequency Ω_j .

A full electromagnetic calculation has been presented in Ref.[94]. It was shown there that the scalar model presented here describes the TE electromagnetic modes inside the cavity. The treatment of TM modes involves an independent scalar field, with a potential proportional to $\delta'(x - L_x/2)$. Moreover, the model has also been generalized to the case of arbitrary positions of the plasma sheet within the cavity [94]. The number of created TE photons depends strongly on the position of the

layer, and the maximum number is attained when it is located at the midpoint of the cavity. On the other hand, for TM modes this dependence is rather weak.

In the treatment above no dissipation effects are considered (the delta-potential is real). Similar calculations for lossless dielectric slabs with time-dependent and real permittivities [93] also neglect dissipation. However, it has been pointed out that dissipative effects may be relevant in the evaluation of created photons [92]. In general, one expects the electromagnetic energy to be dissipated in the cavity walls, in the plasma sheet, and/or in dielectric slabs contained in the cavity. In resonant situations without dissipation, we have seen that the dynamics of the relevant electromagnetic mode is described by a harmonic oscillator with time dependent frequency. A phenomenological way of taking into account dissipative effects is to replace this equation with that of a damped oscillator [95]. Of course this model cannot be consistently quantized unless one includes a noise term, otherwise the usual commutation relations are violated. Using the *quantum noise operator approach* [96] one can estimate the rate of photon creation in this model and, provided the dissipation is not too large, the number of photons still grows exponentially, although at a smaller rate. However, it has been recently argued [38] that these results should be valid only in the short time limit, while in the long time limit the system should reach a stationary state with a constant number of photons inside the cavity. As the calculations in [38] involve 1D cavities, this point deserves further investigation.

5 Experimental perspectives

Since the first theoretical predictions about motion induced radiation, it was clear that the experimental observation of this effect was not an easy task. As mentioned at the end of Section 2, the photon creation produced by a single accelerated mirror is extremely small in realistic situations (see Eq. (20)).

The most promising situation seems to be the photon creation by parametric amplification described in Section 4. However simple numerical estimations show that, even in the most favorable cases, it is difficult to observe the DCE in the laboratory. In all the 3D examples discussed in Section 4, the number of created photons grows exponentially in time as

$$\langle \mathcal{N} \rangle = \sinh^2(\eta \omega \varepsilon t), \quad (85)$$

where ω is the frequency of the resonant mode and η is a number of order 1 related to the geometry of the cavity. Here ε denotes the relative amplitude of the oscillations in the moving mirror case, or the relative amplitude of the oscillations of the relevant component of the wavevector in the case of time dependent conductivity (see Eq.(82)). This equation is valid as long as $\varepsilon^2 \omega t \ll 1$ and neglects any dissipative effects. As the electromagnetic cavity has a finite Q -factor, a rough estimation of the maximum number of created photons $\langle \mathcal{N}_{max} \rangle$ is obtained by setting $t_{max} = Q/\omega$ in the above equation. As mentioned at the end of Section 4, there is

no agreement in the literature about this estimation. Calculations based on the use of a master equation [39] give an exponential growth with a rate diminished by a factor $\Gamma = 1 - 1/(2Q\epsilon)$ (see also Ref. [97]). On the other hand, it was shown that, in the case of 1D cavities, the total number of photons inside the cavity should reach a constant value proportional to the finesse of the cavity at long times [38]. It was argued in the same work that the exponential growth in the presence of dissipation would be valid only at short times. In any case, it is clear that a *necessary* condition to have an observable number of photons is that $2Q\epsilon > 1$.

Assuming a cavity of length $L_0 \simeq 1$ cm, the oscillation frequency of the mirror should be in the GHz range in order to meet the parametric resonance condition. A plausible possibility for reaching such high mechanical oscillation frequencies is to consider surface vibrations, instead of a global motion of the mirror [30]. In this context, the maximum attainable values of the relative amplitude would be around $\epsilon \simeq 10^{-8}$, and therefore the quality factor of the cavity should be greater than 10^8 in order to have a non-negligible number of photons. Microwave superconducting cavities with Q-factors as high as 10^{12} have been built [98]. However, the Q-factor would be severely limited by the presence of an oscillating wall. Therefore, it is an extraordinary challenge to produce extremely fast oscillations while keeping the extremely high Q-factors needed in the DCE. Moreover, the oscillations should be tuned with high precision to parametric resonance with a cavity mode.

5.1 High frequency resonators and photon detection via superradiance

A concrete setup for producing and detecting motion induced photons has been proposed in Ref.[41]. A Film Bulk Acoustic Resonator (FBAR) is a device that consists of a piezoelectric film sandwiched between two electrodes. An aluminum nitride FBAR of thickness corresponding to a half of the acoustic wavelength can be made to vibrate up to a frequency of 3GHz, with an amplitude of $\epsilon = 10^{-8}$. The expected maximum power of Casimir photons produced by such a FBAR depends of course on the Q-factor of the cavity. It can be estimated to be

$$P_{max} = \langle \mathcal{N}_{max} \rangle \hbar \omega / t_{max}. \quad (86)$$

Assuming that $Q\epsilon = O(1)$, this gives $P_{max} \simeq 10^{-22}W$, which is too small for direct detection.

However, this low power could be detected using ultracold atoms. Let us consider a cavity filled with an ensemble of population-inverted atoms in a hyperfine state whose transition frequency is equal to the resonance frequency of the cavity. Then the Casimir photons can trigger a stimulated emission of the atoms, and therefore they can be indirectly detected by this form of *superradiance*. Ref.[41] contains a description of the experimental setup that could be used to observe the DCE, and a discussion about the rejection of signals not produced by the Casimir photons.

In particular, stimulated amplification could also be triggered by the spontaneous decay of one of the atoms (superfluorescence). In order to discriminate between both effects it could be necessary to attain larger values of $Q\varepsilon$.

5.2 *Time dependent conductivity induced by ultra-short laser pulses*

In order to avoid the experimental complications associated with the high frequency motion of the mirror, it is possible to produce effective changes in the length of the cavity by inducing abrupt changes in the reflectivity of a slab contained in the cavity, as already mentioned in Section 4.3. This can be done by illuminating a semiconducting slab with ultra short laser pulses [42, 43]. An experiment based on this idea is currently being carried out by the group of Padova [99].

In this case, a numerical estimation of the maximum number of photons created in the cavity looks, at first sight, much more promising than in the case of moving mirrors. Using a slab of a thickness around 1 mm, it is possible to reach values of ε as large as 10^{-4} , and therefore the constraints on the Q -factor of the cavity are considerably milder. Moreover, it is experimentally possible to generate trains of thousands of laser pulses with a repetition frequency on the order of a GHz.

In Padova's setup (see Fig. 4), a high $Q \approx 10^6$ superconducting cavity contains a GaAs semiconducting slab. The laser pulses are tuned at 4.70 GHz, twice the frequency of the fundamental TE mode of the cavity. However, it has been pointed out [92] that dissipative effects may play an important role in this kind of experiment. Indeed, the changes in the conductivity of the slab are due to the creation of electron-hole pairs by the laser pulses, and during this process the dielectric permittivity acquires an imaginary part. The associated dissipation prevents photon creation unless severe constraints on the properties of the semiconductor are fulfilled: it must have a very short recombination time (tenths of ps), and a high mobility (around $1m^2(Vs)^{-1}$). A slab with these characteristics has been constructed by irradiating a GaAs sample with fast neutrons, in order to reduce the recombination time of the original sample (about 1 ns) while keeping constant the value of the mobility [99]. Photons are detected using a loop antenna inside the cavity. The minimum number of photons that can be detected is around 100, below the expected signal of Casimir photons [47, 99].

A related setup is illumination of a *superconductor* instead of a semiconductor surface. The advantage in this case is that dissipative effects are less important, because the variation of the imaginary part of the permittivity is much smaller for superconductors than for semiconductors in the microwave region [100]. Moreover, since the abrupt changes in the conductivity are due to local heating of the surface (and not to the creation of electron-hole pairs as in the semiconductor), the intensity of the laser can be considerably smaller, reducing unwanted effects of energy accumulation inside the cavity.

5.3 Optical parametric oscillators

Standard nonlinear optics can be interpreted, in some cases, as a time-dependent modulation of the refractive index. Ref. [38] considered an optical parametric oscillator (OPO) with a pump laser beam of frequency Ω and amplitude E_{pump} interacting with a very thin $\chi^{(2)}$ nonlinear crystal slab placed on the interior side of the cavity mirror. For a type-I arrangement, the total polarization component along a suitable crystal symmetry axis may be written in terms of the intracavity electric field component along the same direction as [38]

$$P(t) = \epsilon_0 \left(\chi^{(1)} + \frac{1}{2} \chi^{(2)} E_{\text{pump}} \sin(\Omega t - \theta) \right) E(t), \quad (87)$$

where ϵ_0 is the vacuum permittivity, $\chi^{(1)}$ and $\chi^{(2)}$ are the relevant components of the linear and second-order nonlinear susceptibility tensors, and θ is a phase that depends on the pump beam phase and the position of the crystal.

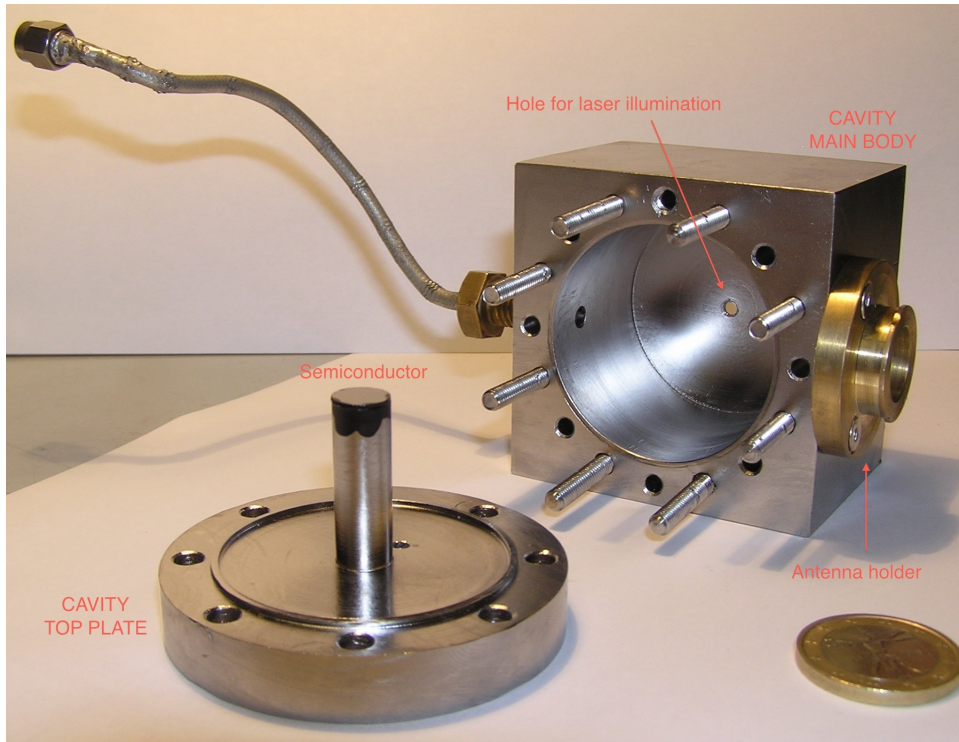


Fig. 4 Superconducting cavity of the experimental setup of MIR experiment at Padova to measure the dynamical Casimir effect (Courtesy of Giuseppe Ruoso).

The total susceptibility as given by eq. (87) (including the nonlinear second-order term) corresponds to an effective refractive index oscillating at the pump beam frequency Ω , thus leading to a modulation of the optical cavity length. This is formally equivalent to modulating the physical cavity length by bouncing the mirror with frequency Ω . But in the OPO the pump beam frequency is in the optical range, as are the generated photons with frequencies satisfying $\omega + \omega' = \Omega$. For ω and ω' corresponding to cavity modes, parametric amplification is enhanced and the resulting photon flux is typically several orders of magnitude higher than in the case of mechanical motion [38].

5.4 Superconducting coplanar waveguides

Another possibility to induce fast variations of the b.c. on the electromagnetic field is to consider a coplanar waveguide terminated by a SQUID [49, 50]. A time-dependent magnetic flux can be applied to control the effective inductance of the SQUID, which in turn produces a time-dependent Robin boundary condition for the phase field (time integral of the electric field), equivalent to that of a transmission line with a variable length. This setup simulates a moving Robin mirror in 1D with an effective velocity that might be close to the speed of light. As a consequence, the first-order non-relativistic results [22, 64], based on the perturbative approach outlined in Section 2, must be modified by the inclusion of higher-order frequency sidebands [49].

As in the previous examples, it is crucial to check if the flux of Casimir photons can be discriminated from other sources of photons, like the classical thermal contribution. The analysis presented in Ref.[49] shows that this is the case, for realistic values of the parameters, at temperatures below 70 mK.

6 Final remarks

We have reviewed some theoretical and experimental advances in the analysis of moving bodies or time dependent boundary conditions coupled to the vacuum fluctuations of the electromagnetic field.

Accelerated neutral bodies produce the emission of real photons, while experiencing a radiation reaction force. When the dynamics of the bodies is treated quantum mechanically, the interaction with the vacuum fluctuations not only causes this dissipative force, but also an appreciable amount of decoherence, which is a consequence of the entanglement between the mirrors and the electromagnetic field. This is a particular example of quantum Brownian motion, where the Brownian particle (mirror) loses coherence while being subjected to a damping force due to its coupling to the environment (the quantum field).

When two neutral bodies are in relative motion, we expect velocity-dependent forces between them. There is a particularly interesting situation in which two parallel, non-perfectly conducting slabs are in relative parallel motion with constant velocity. In this case, there is a *vacuum friction* between the slabs even in the absence of real photons. The effect can be understood in terms of the interaction of image charges, or as the interchange of virtual photons between the surfaces. There are similar friction forces for neutral atoms moving near surfaces.

The rate of photon creation produced by a single accelerated body in free space is deceptively small in realistic situations. However, in closed cavities a much larger number of photons may be produced by parametric amplification. Indeed in an ideal 3D cavity one expects an exponential growth in the number of photons when its size varies periodically at an appropriate resonant frequency, making detection of photon creation not an impossible task. The calculation of photon creation in the presence of ideal conductors have been performed in 1D and 3D using different analytical approximations. The results are consistent and have been confirmed by fully numerical calculations. However, the case of moving mirrors with finite conductivity (i.e electromagnetic cavities with a finite Q -factor) is not a completely settled issue. In 1D cavities, at short times the growth of the total number of created photons is still exponential (with a different rate), while at large times the total number of photons should reach saturation. This problem has not yet been solved for 3D cavities. The difficulties in evaluating the DCE for mirrors with finite conductivity recalls a similar situation in the static Casimir effect, where the evaluation of the Casimir force depends strongly on the theoretical model used to describe the conductivity of the bodies, and there are interesting correlations between finite conductivity, temperature and geometry. These correlations may have relevant counterparts in the dynamical problem. In any case, although difficult, the direct experimental detection of the motion induced radiation is not out of reach, as long as one can keep a very high Q -factor in a cavity with moving walls. In particular, there is a specific proposal that involves nanoresonators in a high Q -cavity filled with a gas of cold atoms to detect a small number of photons through superradiance.

An exponentially large number of photons can also be produced when some electromagnetic property of the cavity varies periodically with time. Of particular importance is the case in which the conductivity of a semiconductor or superconductor slab placed inside an electromagnetic cavity is modulated using short laser pulses. Theoretical estimates show that this setup could be implemented, with milder requirements on the Q -factor of the cavity. Once again, there is no comprehensive theoretical model that takes into account the (dissipative) response of the slab to the laser pulses, and its relevance for the photon creation process. However, this is a promising alternative and there is an ongoing experiment at Padova based on this setup.

There are other possibilities to produce fast variations of the boundary conditions on the electromagnetic field, that involve optical parametric oscillators or superconducting waveguides. The theoretical analyses suggest that it should be easier to detect the photons created in these setups than in the case of moving mirrors.

In summary, there is a plethora of interesting effects related to the electromagnetic vacuum fluctuations in the presence of moving bodies and/or other time dependent external conditions. The eventual experimental confirmation of some of these effects will certainly produce an increasing activity on this subject in the near future, as was the case for the static Casimir effect following the first realization of precise experiments in that area since 1997.

Acknowledgements The work of DARD was funded by DARPA/MTO's Casimir Effect Enhancement program under DOE/NNSA Contract DE-AC52-06NA25396. PAMN thanks CNPq and CNE/FAPERJ for financial support and the Universidad de Buenos Aires for its hospitality during his stay at Buenos Aires. FDM thanks the Universidad de Buenos Aires, CONICET and ANPCyT for financial support. We are grateful to Giuseppe Ruoso for providing a picture of MIR experiment at Padova.

References

1. Barton, G.: On the fluctuations of the Casimir force. *J. Phys. A: Math. Gen.* **24**, 991-1005 (1991)
2. Barton, G.: On the fluctuations of the Casimir force. 2: the stress-correlation function. *J. Phys. A: Math. Gen.* **24**, 5533-5551 (1991)
3. Jaekel, M.-T. and Reynaud, S.: Quantum fluctuations of position of a mirror in vacuum. *J. Phys. (Paris) I* **3**, 1-20 (1993)
4. Dalvit, D. A. R. and Maia Neto, P. A.: Decoherence via the Dynamical Casimir Effect. *Phys. Rev. Lett.* **84**, 798-801 (2000); Maia Neto, P. A. and Dalvit, D. A. R.: Radiation pressure as a source of decoherence *Phys. Rev. A* **62**, 042103 (2000).
5. Callen, H. B. and Welton, T. A.: Irreversibility and generalized noise. *Phys. Rev.* **83**, 34-40 (1951)
6. Ford, L. H. and Vilenkin, A.: Quantum radiation by moving mirrors. *Phys. Rev. D* **25**, 2569-2575 (1982).
7. Moore, G. T.: Quantum theory of electromagnetic field in a variable-length one-dimensional cavity. *J. Math. Phys.* **11**, 2679 (1970).
8. Castagnino, M. and Ferraro, R.: The radiation from moving mirrors: The creation and absorption of particles. *Ann. Phys. (NY)* **154**, 1-23 (1984)
9. Fulling, S. A. and Davies, P. C. W.: Radiation from a moving mirror in two dimensional space-time - conformal anomaly. *Proc. R. Soc. A* **348**, 393-414 (1976).
10. Hawking, S. W.: Black-hole explosions. *Nature (London)* **248**, 3031 (1974); Particle creation by black-holes. *Commun. Math. Phys.* **43**, 199220 (1975)
11. Braginsky, V. B. and Khalili, F. Ya.: Friction and fluctuations produced by the quantum ground-state. *Phys. Lett* **161**, 197-201 (1991).
12. Jaekel, M.-T. and Reynaud, S.: Fluctuations and dissipation for a mirror in vacuum. *Quantum Opt.* **4**, 39-53 (1992).
13. Braginsky, V. B. and Vorontsov, Yu. I.: Quantum-mechanical limitations in macroscopic experiments and modern experimental techniques. *Usp. Fiz. Nauk.* **114**, 41-53 (1974); Caves, C.: Defense of the standard quantum limit for free-mass position. *Phys. Rev. Lett.* **54**, 2465-2468 (1985); Jaekel, M.-T. and Reynaud, S.: Quantum limits in interferometric measurements. *Europhys. Lett.* **13**, 301-306 (1990)
14. Kubo, R.: Fluctuation-dissipation theorem. *Rep. Prog. Phys.* **29**, 255-284 (1966)

15. Maia Neto, P. A. and Reynaud, S.: Dissipative force on a sphere moving in vacuum. *Phys. Rev. A* **47**, 1639-1646 (1993)
16. Barton, G.: New aspects of the Casimir effect: fluctuations and radiative reaction, in *Cavity Quantum Electrodynamics*, Supplement: Advances in Atomic, Molecular and Optical Physics, edited by P. Berman, (Academic Press, New York, 1993)
17. Maia Neto, P. A. and Machado, L. A. S.: Radiation Reaction Force for a Mirror in Vacuum. *Braz. J. Phys.* **25**, 324-334 (1995)
18. Golestanian, R. and Kardar, M.: Mechanical Response of Vacuum. *Phys. Rev. Lett.* **78**, 3421-3425 (1997); *Phys. Rev. A* **58**, 1713-1722 (1998)
19. Volotikin, A. I. and Persson, B. N. J.: Near-field radiative heat transfer and noncontact friction. *Rev. Mod. Phys.* **79**, 1291-1329 (2007)
20. Pendry, J. B.: Shearing the vacuum - quantum friction. *J. Phys.:Condens. Matter* **9**, 10301-10320 (1997)
21. Nussenzveig, H. M.: Causality and dispersion relations (Academic Press, New York, 1972).
22. Lambrecht, A., Jaekel, M.-T. and Reynaud, S.: Motion induced radiation from a vibrating cavity. *Phys. Rev. Lett.* **77**, 615-618 (1996)
23. Maia Neto, P. A. and Machado, L. A. S.: Quantum radiation generated by a moving mirror in free space. *Phys. Rev. A* **54**, 3420-3427 (1996)
24. Montazeri, M. and Miri, M.: Radiation from a dynamically deforming mirror immersed in the electromagnetic vacuum. *Phys. Rev. A* **77**, 053815 (2008)
25. Mundarain, D. F. and Maia Neto, P. A.: Quantum radiation in a plane cavity with moving mirrors. *Phys. Rev. A* **57**, 1379-1390 (1998).
26. Maia Neto, P. A.: The dynamical Casimir effect with cylindrical waveguides. *J. Opt. B: Quantum Semiclass. Opt.* **7**, S86S88 (2005)
27. Pascoal, F., Celeri, L. C., Mizrahi, S. S. and Moussa, M. H. Y.: Dynamical Casimir effect for a massless scalar field between two concentric spherical shells. *Phys. Rev. A* **78**, 032521 (2008); Pascoal, F., Celeri, L. C., Mizrahi, S. S., Moussa, M. H. Y. and Farina, C.: Dynamical Casimir effect for a massless scalar field between two concentric spherical shells with mixed boundary conditions. *Phys. Rev. A* **80**, 012503 (2009)
28. Eberlein, C.: Theory of quantum radiation observed as sonoluminescence. *Phys. Rev. A* **53**, 2772-2787 (1996)
29. Mazzitelli, F. D. and Millán, X. O.: Photon creation in a spherical oscillating cavity. *Phys. Rev. A* **73**, 063829 (2006).
30. Dodonov, V. V. and Klimov, A. B.: Generation and detection of photons in a cavity with a resonantly oscillating boundary, *Phys. Rev. A* **53**, 2664-2682 (1996)
31. Crocce, M., Dalvit, D. A. R. and Mazzitelli, F. D.: Resonant photon creation in a three dimensional oscillating cavity, *Phys. Rev. A* **64**, 013808 (2001)
32. Crocce, M., Dalvit, D. A. R. and Mazzitelli, F. D.: Quantum electromagnetic field in a three dimensional oscillating cavity, *Phys. Rev. A* **66**, 033811 (2002)
33. Crocce, M., Dalvit, D. A. R., Lombardo, F. and Mazzitelli, F. D.: Hertz potentials approach to the dynamical Casimir effect in cylindrical cavities of arbitrary section. *J. Opt. B: Quantum Semiclass. Opt.* **7**, S32-S39 (2005)
34. Dalvit, D. A. R. and Mazzitelli, F. D.: Renormalization-group approach to the dynamical Casimir effect. *Phys. Rev. A* **57**, 2113-2119 (1998)
35. Lambrecht, A., Jaekel, M.-T. and Reynaud, S.: Frequency up-converted radiation from a cavity moving in vacuum. *Eur.Phys.J. D* **3** 95-104 (1998)
36. Dalvit, D. A. R. and Mazzitelli, F. D.: Creation of photons in an oscillating cavity with two moving mirrors. *Phys. Rev. A* **59**, 3049-3059 (1999)
37. Jaekel, M.-T. and Reynaud, S.: Motional Casimir force. *J. Phys. I* **2** 149-165 (1992).
38. Dezael, F. X. and Lambrecht, A.: Analogue Casimir radiation using an optical parametric oscillator. *Europhys. Lett.* **89**, 14001 (2010)
39. Dodonov, V. V.: Dynamical Casimir effect in a nondegenerate cavity with losses and detuning. *Phys. Rev. A* **58**, 4147-4152 (1998)
40. Schaller, G., Schützhold, R., Plunien, G. and Soff, G.: Dynamical Casimir effect in a leaky cavity at finite temperature. *Phys. Rev. A* **66**, 023812 (2002)

41. Kim, W.-J., Brownell, J. H. and Onofrio, R.: Detectability of dissipative motion in quantum vacuum via superradiance. *Phys. Rev. Lett.* **96**, 200402 (2006)
42. Yablonovitch, E.: Accelerating reference frame for electromagnetic waves in a rapidly growing plasma: Unruh-Davies-Fulling-DeWitt radiation and the nonadiabatic Casimir effect. *Phys. Rev. Lett.* **62**, 1742-1745 (1989) Yablonovitch, E., Heritage, J. P., Aspnes, D. E. and Yafet, Y.: Virtual photoconductivity, *Phys. Rev. Lett.* **63**, 976-979 (1989)
43. Lozovik Y. E., Tsvetus, V. G. and Vinogradov, E. A.: Femtosecond parametric excitation of electromagnetic field in a cavity. *JETP Lett.* **61**, 723-729 (1995) Parametric excitation of vacuum by use of femtosecond laser pulses, *Phys. Scr.* **52**, 184-190 (1995)
44. Croce, M., Dalvit, D. A. R., Lombardo, F. and Mazzitelli, F. D.: Model for resonant photon creation in a cavity with time dependent conductivity, *Phys. Rev. A* **70**, 033811 (2004)
45. Mendonça, J. T. and Guerreiro, A.: *Phys. Rev. A* **80**, 043603 (2005)
46. Braggio, C. *et al*: A novel experimental approach for the detection of the dynamic Casimir effect. *Europhys. Lett.* **70**, 754-760 (2005)
47. Braggio, C. *et al*: Characterization of a low noise microwave receiver for the detection of vacuum photons. *Nuclear Instruments and Methods in Physics Research A* **603**, 451-455 (2009)
48. Takashima, K. *et al*: Nonstationary boundary effect for a quantum flux in superconducting nanocircuits. *J. Phys. A* **41**, 164036 (2008); Castellanos-Beltran, M. A *et al*: Amplification and squeezing of quantum noise with a tunable Josephson metamaterial. *Nat. Phys.* **4**, 928-931 (2008)
49. Johansson, J. R. , Johansson, G., Wilson, C. M. and Nori, F.: Dynamical Casimir effect in a superconducting coplanar waveguide, *Phys. Rev. Lett.* **103**, 147003 (2009)
50. Wilson, C. M., Duty, T., Sandberg, M., Persson, F., Shumeiko, V. and Delsing, P.: Photon generation in an electromagnetic cavity with a time-dependent boundary, arXiv:1006.2540
51. Carusotto, I., Balbinot, R., Fabbri, A. and Recati, A.: Density correlations and analog dynamical Casimir emission of Bogoliubov phonons in modulated atomic Bose-Einstein condensates. *European Phys. J. D* **56**, 391-404 (2010)
52. Roberts, D. and Pomeau, Y.: Casimir-like force arising from quantum fluctuations in a slow-moving dilute Bose-Einstein condensate. *Phys. Rev. Lett.* **95** 145303 (2005)
53. Jaekel, M.-T. and Reynaud, S.: Movement and fluctuations of the vacuum. *Rep. Prog. Phys.* **60** 863-887 (1997)
54. Kardar, M. and Golestanian, R.: The "friction" of vacuum, and other fluctuation-induced forces. *Rev. Mod. Phys.* **71**, 1233-1245 (1999)
55. Dodonov, V. V.: Nonstationary Casimir effect and analytical solutions for quantum fields in cavities with moving boundaries. *Advances Chem. Phys.* **119**, 309-394 (2001)
56. Dodonov, V.V.: Dynamical Casimir effect: Some theoretical aspects *J. Phys.: Conf. Ser.* **161** 012027 (2009)
57. Dodonov, V. V.: Current status of the dynamical Casimir effect. arXiv:1004.3301 (2010)
58. Fosco, C. D, Lombardo, F. C. and Mazzitelli, F. D.: Quantum dissipative effects in moving mirrors: a functional approach *Phys. Rev. D* **76**, 085007 (2007).
59. Barton, G. and Eberlein, C.: On quantum radiation from a moving body with finite refractive-index. *Ann. Phys. (N.Y.)* **227**, 222-274 (1993)
60. Alves, D. T., Farina, C. and and Maia Neto, P. A., Dynamical Casimir effect with Dirichlet and Neumann boundary conditions. *J. Phys. A: Math. Gen.* **36**, 11333-11342 (2003)
61. Alves, D. T., Granhen, E. R. and Lima, M. G.: Quantum radiation force on a moving mirror with Dirichlet and Neumann boundary conditions for a vacuum, finite temperature, and a coherent state. *Phys. Rev. D* **77**, 125001 (2008)
62. Mintz, B., Farina, C., Maia Neto, P. A. and Rodrigues, R.: Casimir forces for moving boundaries with Robin conditions. *J. Phys. A: Math. Gen.* **39**, 6559-6565 (2006)
63. Dodonov, V. V., Klimov, A. B. and Man'ko, V. I.: Generation of squeezed states in a resonator with a moving wall. *Phys. Lett. A* **149**, 225-228 (1990); Dodonov, V. V. and Klimov, A. B.: Long-time asymptotics of a quantized electromagnetic-field in a resonator with oscillating boundary. *Phys. Lett. A* **167**, 309-313 (1992)

64. Mintz, B., Farina, C., Maia Neto, P. A. and Rodrigues, R.: Particle creation by a moving boundary with a Robin boundary condition. *J. Phys. A: Math. Gen.* **39**, 11325-11333 (2006)
65. Jaekel, M.-T. and Reynaud, S.: Causality, stability and passivity for a mirror in vacuum. *Phys. Lett. A* **167**, 227-232 (1992)
66. Barton, G. and Calogeracos, A.: On the quantum electrodynamics of a dispersive mirror. 1: Mass shifts, radiation, and radiative reaction. *Ann. Phys. (N.Y.)* **238**, 227-267 (1995)
67. Verlot, P., Tavernarakis, A., Briant, T., Cohadon, P. -F. and Heidmann, A.: Scheme to probe optomechanical correlations between two optical beams down to the quantum level. *Phys. Rev. Lett.* **102**, 103601 (2009); Schliesser, A., Arcizet, O., Riviere, R., Anetsberger, G., Kippenberg T. J.: Resolved-sideband cooling and position measurement of a micromechanical oscillator close to the Heisenberg uncertainty limit. *Nature Phys.* **5**, 509-514 (2009).
68. Maia Neto, P. A.: Vacuum radiation pressure on moving mirrors. *J. Phys. A: Math. Gen.* **27**, 2167-2180 (1994)
69. Barton G. and North C. A.: Peculiarities of Quantum Radiation in Three Dimensions from Moving Mirrors with High Refractive Index. *Ann. Phys. (N.Y.)* **252**, 72-114 (1996)
70. Gütig, R. and Eberlein, C.: Quantum radiation from moving dielectrics in two, three and more spatial dimensions. *J. Phys. A: Math. Gen.* **31**, 6819-6838 (1998).
71. Barton, G.: The quantum radiation from mirrors moving sideways. *Ann. Phys. (N.Y.)* **245**, 361-388 (1996).
72. Pendry, J. B.: Quantum friction – fact or fiction ? *New J. Phys.* **12**, 033028 (2010).
73. Volotikin, A. I. and Persson, B. N. J.: Theory of friction: the contribution from a fluctuating electromagnetic field. *J. Phys.:Condens. Matter* **11**, 345-359 (1999)
74. Lifshitz, E. M.: The theory of molecular attractive forces between solids. *Sov. Phys. JETP* **2**, 73-83 (1956)
75. Buhmann, S. Y and Welsch, D.-G.: Dispersion forces in macroscopic quantum electrodynamics. *Progress in Quantum Electronics* **31**, 51-130 (2007)
76. Dedkov, G. V. and Kyasov, A. A.: Electromagnetic and fluctuation-electromagnetic forces of interaction of moving particles and nanoprobes with surfaces: a non-relativistic consideration. *Physics of the Solid State* **44**, 1809-1832 (2002)
77. Hu, B. L., Roura, A., and Shresta, S.: Vacuum fluctuations and moving atom/detectors: from the Casimir-Polder to the Unruh-Davies-DeWitt-Fulling effect. *J. Opt. B: Quantum Semiclass. Opt.* **6**, S698-S705 (2004)
78. Scheel, S. and Buhmann, S. Y.: Casimir-Polder forces on moving atoms. *Phys. Rev. A* **80**, 042902 (2009)
79. Dodonov, V. V., Klimov, A. B. and Nikonov, D. E.: Quantum phenomena in resonators with moving walls. *J. Math. Phys.* **34**, 2742 (1993)
80. Petrov, N. P. : The dynamical Casimir effect in a periodically changing domain: a dynamical systems approach. *J. Opt B: Quant. Semiclass. Optics* **7**, S89-S99 (2005)
81. Ruser, M.: Vibrating cavities: a numerical approach. *J. Opt. B: Quant. Semiclass. Optics* **7**, S100-S115 (2005)
82. Alves, D. T., Farina, C. and Granhen, E. R.: Dynamical Casimir effect in a resonant cavity with mixed boundary conditions. *Phys. Rev. A* **73**, 063818 (2006)
83. Farina, C., Pascoal, F. and Azevedo, D.: Dynamical Casimir effect with Robin boundary conditions in a three dimensional open cavity. arXiv:1001.2530. To appear in the Proceedings of QFEXT09 (2010)
84. Law, C. K.: Resonance response of the quantum vacuum to an oscillating boundary. *Phys. Rev. Lett.* **73**, 1931-1934 (1994)
85. Schützhold, R., Plunien, G. and Soff, G.: Trembling cavities in the canonical approach. *Phys.Rev. A* **57**, 2311-2318 (1998)
86. Bender, C. M. and Orszag, S.A.: *Advanced Mathematical Methods for Scientists and Engineers* (McGraw Hill, New York, 1978)
87. Boyd, R.: *Nonlinear Optics* (Academic Press, Burlington USA, 2008) (third edition)
88. Ji, J.-Y., Soh, K.-S., Cai, R.-G. and Kim, S. P.: Electromagnetic fields in a three-dimensional cavity and in a waveguide with oscillating walls. *J. Phys. A* **31**, L457-L462 (1998)

89. Dodonov, V. V.: Resonance excitation and cooling of electromagnetic modes in a cavity with an oscillating wall. *Phys. Lett. A* **213**, 219-225 (1996)
90. M. Ruser: Numerical investigation of photon creation in a three-dimensional resonantly vibrating cavity: Transverse electric modes, *Phys. Rev. A* **73**, 043811 (2006).
91. Hacyan, S., Jauregui, R., Soto, F. and Villarreal, C: Spectrum of electromagnetic fluctuations in the Casimir effect. *J. Phys. A: Math. Gen.* **23**, 2401 (1990)
92. Dodonov, V. V. and Dodonov, A.V.: The nonstationary Casimir effect in a cavity with periodical time-dependent conductivity of a semiconductor mirror. *J. Phys. A: Math. Gen.* **39**, 6271-6281 (2006)
93. Uhlmann, M., Plunien, G., Schützhold, R. and Soff, G.: Resonant cavity photon creation via the dynamical Casimir effect. *Phys. Rev. Lett.* **93**, 193601 (2004)
94. Naylor, W., Matsuki, S., Nishimura, T. and Kido, Y.: Dynamical Casimir effect for TE and TM modes in a resonant cavity bisected by a plasma sheet, *Phys. Rev. A* **80**, 043835 (2009)
95. Dodonov, V. V.: Photon distribution in the dynamical Casimir effect with an account of dissipation, *Phys. Rev. A* **80**, 023814 (2009)
96. Lax, M.: Quantum noise. IV. Quantum theory of noise sources, *Phys. Rev.* **145**, 110-129 (1966)
97. Mendonça, J.T. , Brodin, G., and Marklund, M.: Vacuum effects in a vibrating cavity: time refraction, dynamical Casimir effect, and effective Unruh acceleration. *Phys. Lett. A* **372**, 5621-5624 (2008).
98. Arbert-Engels, V. *et al*: Superconducting niobium cavities, a case for the film technology. *Nucl. Instrum. Methods Phys. Res. A* **463**, 1-8 (2001)
99. Agnesi, A. *et al*: MIR status report: an experiment for the measurement of the dynamical Casimir effect. *J. Phys. A: Math. Gen.* **41**, 164024 (2008).
100. Segev, E. *et al*: Prospects of employing superconducting stripline resonators for studying the dynamical Casimir effect experimentally. *Phys. Lett. A* **370**, 202-206 (2007).